THE PRODUCTION OF A STANDARD MATERIAL FOR LIBERATION ANALYSIS

David Lin

A thesis submitted to the

Faculty of Graduate Studies and Research

in partial fulfillment of the requirements

for the degree of Master of Engineering

Department of Mining and Metallurgical Engineering

McGill University, Montreal

ABSTRACT

In mineral processing, the liberation distribution of the mineral phases in an ore is an important factor. Unfortunately, liberation distribution is very difficult to measure accurately. One problem is the stereological effect associated with a microscopic liberation analysis.

Many methods have been proposed to correct for the stereological effect, but they remain essentially untested, in part due to the lack of a standard or reference material. In this work, a method was established to create an artificial standard material.

Silica grains were placed in an epoxy resin to create a block of material that was crushed to yield liberated and locked particles. The composition, and thus liberation, of these particles was determined with a series of heavy liquid separations.

By changing the grain size to particle size ratio, the type and amount of locking was affected. The best compromise between the amount of locked material produced and the production of simple locked particles (which pose the greatest stereological challenge) was found; it occurred at the point where the grain and particle sizes were the same.

Liberation analyses were performed on this material and compared with a model prediction based on the sectioning of spheres with single planar interfaces. There were some discrepancies between the analysis and model results.

RÉSUMÉ

En minéralurgie, la distribution de la libération des phases minerals dans un minerai est un facteur important. Malheureusement, il est très difficile de quantifier avec précision la distribution de la libération de ces phases. L'effet stéréologique qui est associé à une analyse de libération par microscopie est un des problèmes.

Plusieurs méthodes ont été proposées afin de corriger cet effet stéréologique, mais elles demeurent pratiquement non vérifiées, dû en partie a l'absence d'un matériel standard ou de référence. Pour ce travail, on a mis au point une méthode pour créer, artificiellement, un matériel standard.

Des grains de silice furent déposés dans une résine d'époxy pour creer un bloc de matériel qui fut ensuite concassé, produisant ainsi des particules libres et des mixtes. La composition, d'où la libération de ces particules, fut déterminee par une suite de séparation par liquids lourds.

En changeant le ratio entre la dimension des grains et celle des particules, le type et la quantité de matériel non-libéré furent affectés. On a ainsi trouvé le meilleur compromis entre la quantité de matériel non-libre produit et la production de mixtes simples (ce qui pose le plus grand défi en stéréologie); ce dernier se retrouve où la dimension des grains et des particules est la même.

On a effectué des analyses de libération sur ce matériel et on les a

comparées à celles d'un modèle ayant comme principe le sectionnement de sphères à interfaces planaires simples. On a noté certaines différences entre les résultats des analyses et ceux du modèle.

ACKNOWLEDGEMENTS

I wish to acknowledge the help and guidance of Professor James Finch and Dr. Cesar Gomez throughout the course of this work. Their advice, without which this work would not have been possible, is greatly appreciated. I would also like to thank Professor André Laplante, S. Banisi and the other members of the mineral processing group for their helpful input.

A special thanks to Michel Leroux for his help in the laboratory. Thanks also go to CANMET and Dr. W. Petruk for the image analysis of my samples and finally, to Energy, Mines and Resources, Canada (Research Agreements Program) for providing the funding for this project.

TABLE OF CONTENTS

GLOSSARY

ARTIFACT : general name for a particle section whose composition differs from that of the original particle.

COMPLEX LOCKING : locking such that there is more than one interface between the phases in the locked particle.

COMPOSITE PARTICLE : a locked particle.

DEGREE OF LIBERATION : ratio of the volume of free particles of a certain phase to the total volume of that phase.

DETACHMENT : breakage at an interface due to mineral boundary weaknesses

DILUENT (OR FILLER) MATERIAL : particles of a material deliberately introduced into a sample to reduce the incidence of contact between particles.

FRECKLING : the embedding of fine silica into the resin surface during the grinding process.

FREE (OR LIBERATED) PARTICLE : a particle consisting of only one mineral phase.

GRAIN : a mineral feature in the matrix before comminution.

HALO : the variation in the intensity level around the edges of the electron microscope image of a particle section caused by the averaging effect of the signal in the interaction volume. Halos make phase boundaries difficult to discriminate

INTERACTION VOLUME : the part of the sample which produces signals when

excited by the electron beam of an electron microscope.

LIBERATION : the freeing of a mineral phase from its associated matrix.

LIBERATION DISTRIBUTION : the amount (volume or mass) of material in each particle composition class for a given phase.

LINEAR LIBERATION ANALYSIS : the determination of the liberation distribution by measuring the intercepts of linear probes through the sample.

LOCKING : the occurrence of particles consisting of more than one mineral phase.

MATRIX : the material that surrounds the mineral grains before comminution.

MATRIX RESIN : the resin that is used to support grains of silica in the silica/resin blocks and forms one of the phases of the standard material.

MOUNTING MEDIUM : the material (usually resin) that is used to hold the particles in space so they can be sectioned and examined under a microscope.

PARTICLE : the fragments of material that result from comminution.

PREFERENTIAL BREAKAGE : the increased breakage rate of a certain phase in an ore compared to the other phases.

PRIMARY BINARY IMAGE : the binary image of a specific mineral phase created from the secondary grey image.

PRIMARY GREY IMAGE : the image from the electron microscope that is obtained by the image analyzer upon which image processing will be performed.

RESOLUTION : the ability of the microscope to discriminate accurately the smaller features in a sample.

SECONDARY BINARY IMAGE : the image that results after binary filters have

been applied to the primary binary image.

SECONDARY GREY IMAGE : the image that results after grey level filters have been applied to the primary grey image.

SIMPLE LOCKING : locking such that there is only one interface between the phases in a locked particle.

STANDARD MATERIAL : a material of known liberation and composition exhibiting liberated and simple locked behaviour.

STEREOLOGICAL EFFECT : a bias which creates an overestimation of liberation in microscopic liberation analyses.

LIST OF FIGURES

LIST OF TABLES

THE PRODUCTION OF A STANDARD MATERIAL FOR LIBERATION ANALYSIS

1. INTRODUCTION

1.1 Background

The efficient and economic recovery of valuable minerals from raw ore depends on several factors. In the primary stages of separation, the most important factor is comminution, the crushing and grinding of the ore. The ore has to be reduced in size so that the valuable minerals occur as so-called liberated or free particles. This is the process of liberation.

Ignoring the role of particle size for the moment, it can be said that the larger the fraction of the mineral phase that occurs as free particles or the higher the degree of liberation, the more successful will be the separation. While a high degree of liberation is desirable, a comminution system that produces only free

particles is difficult if not impossible to achieve.

It has been stated that complete liberation can never be theoretically achieved if only random breakage is assumed. Meloy's theory of constant interfacial area [1] states that the area of locking between the different phases will remain constant regardless of the amount of comminution performed if liberation by detachment does not occur. This is intuitive because the chances of a random fracture occurring along an interface is very small. Of course, this does not imply that a satisfactory degree of liberation cannot be obtained. With comminution, the mass of mineral locked in composite particles is reduced so that their rejection may translate to an economically acceptable loss in recovery. Also, in practice, liberation by detachment may play a significant role in increasing the degree of liberation [2].

Extensive comminution will reduce the size of the particles and subsequently increase the chance for liberation to occur. This, however, creates two problems. Firstly, comminution is a very energy intensive operation. The cost of comminution can contribute up to 50% of the mill operating cost [3] and, therefore, there are economic constraints on the amount of comminution that can be done. Secondly, the production of very fine particles due to large amounts of comminution is a problem because fine particles are more difficult to separate than coarse ones [4]. An optimum amount of particle size reduction has to be found.

In order to determine the point at which comminution has to cease and

separation begin, knowledge of the liberation distribution is desirable. Unfortunately, this is a very difficult task to accomplish accurately. Liberation models [2,5,6,7] cannot yet characterize the texture and breakage of complex ores to give useful predictions of liberation. Therefore, the liberation distribution has to be measured. Presently, this is usually done by microscopic examination, but there is an inherent error in all measurements made in this manner.

The microscopic examination of particulates is done by randomly dispersing the particles in a resin mounting medium from which a surface is cut and polished. This produces a polished surface which can be examined with an optical or electron microscope. The liberation distribution is measured by determining the percentage of the relevant mineral in the different particle sections. With the advent of computerized image analyzers, the measurement of the liberation distribution has become quicker and more precise than before, but not necessarily more accurate. An image analyzer is simply a computer software package that measures certain particle properties from the digitized image of the polished surface produced by an electron microscope or optical microscope camera. A scanning electron microscope (SEM) and an electron microprobe (MP) will be used in this study.

Unfortunately, the measurement of the liberation distribution using a polished surface is biased because a sectional view of the particles gives only two-dimensional information and liberation is a three-dimensional variable. Sectional liberation data has to be corrected to yield a measure of the true liberation distribution.

Several correction algorithms have been proposed. They are all essentially untested since a sample of known liberation distribution (i.e. a standard material) is not available.

1.2 Thesis Objective

The objective of this work is the development of a method to produce a standard material for liberation analysis. This standard material will allow an assessment of the effectiveness of the various stereological correction methods proposed by different researchers.

2. LIBERATION ANALYSIS

2.1 Objective

The objective of a liberation analysis is to provide quantitative and qualitative information about the liberation characteristics of a stream of mineral particles. A standard procedure to produce liberation data has yet to be established, but with careful sample preparation and analysis, useful results can be obtained. A short overview of the procedure and equipment of a liberation analysis is presented below.

2.2 Sample Preparation

The preparation of a sample for liberation analysis involves several steps :

1) subsampling
2) screening
3) particle mounting
4) polishing.

Each step of this procedure must be performed with care. Poor sample preparation can lead to the production of polished surfaces that are unrepresentative of the

original sample.

2.2.1 Subsampling

Only a small amount of material can be examined in a microscopic liberation analysis and, therefore, accurate reduction of the mass of the sample is necessary. There is a great quantity of literature on this subject, but this falls outside the scope of this thesis and it will be assumed that subsampling is correctly performed following an accepted method [8].

2.2.2 Screening

It is necessary to screen the sample into size intervals and mount each size fraction separately because a liberation analysis should be done on a size by size basis [9, p.18]. This provides information about how the liberation distribution varies with particle size. Screening is also important because when a particle is sectioned, there is a distribution of section sizes. If the samples were not screened, it would be impossible to distinguish whether a particle section is the same size as the original particle or if it was the result of the sectioning of a larger particle. In addition, it is difficult to analyze particles of different sizes in the same polished surface because the resolution may be too poor to allow the discrimination of small particles if very large particles are present in the same

image. In the analysis in this study, the particles in each sample will consist only of one $\sqrt{2}$ Tyler size class.

2.2.3 Particle Mounting

After subsampling and screening have been performed, it is important that the particles of the sample be dispersed randomly in the mounting medium. This is important because the polished surface that will be examined must be representative of the original sample. Due to the initial liquid nature of the mounting medium, the particles tend to settle preferentially (due to differences in mineral density and particle shape) before the medium can harden. This segregation of the particles in the mounting medium can create a bias in the sectioning results. For example, heavier particles may be over-represented if a section is polished near the bottom of the sample and lighter particles will be over-represented if a section is polished near the top (Figure 2.1). Many methods have been suggested to overcome the segregation problem, but none of them have proven to be completely successful [10].

Air bubbles and other voids that might be introduced into the sample must be avoided as well. When the sample is polished, they will inevitably trap polishing residue as well as material removed from the sample [11]. This can cause false particle occurrences when the sample is examined under the microscope. The particle mounting method used in this work is explained in Section 5.2.

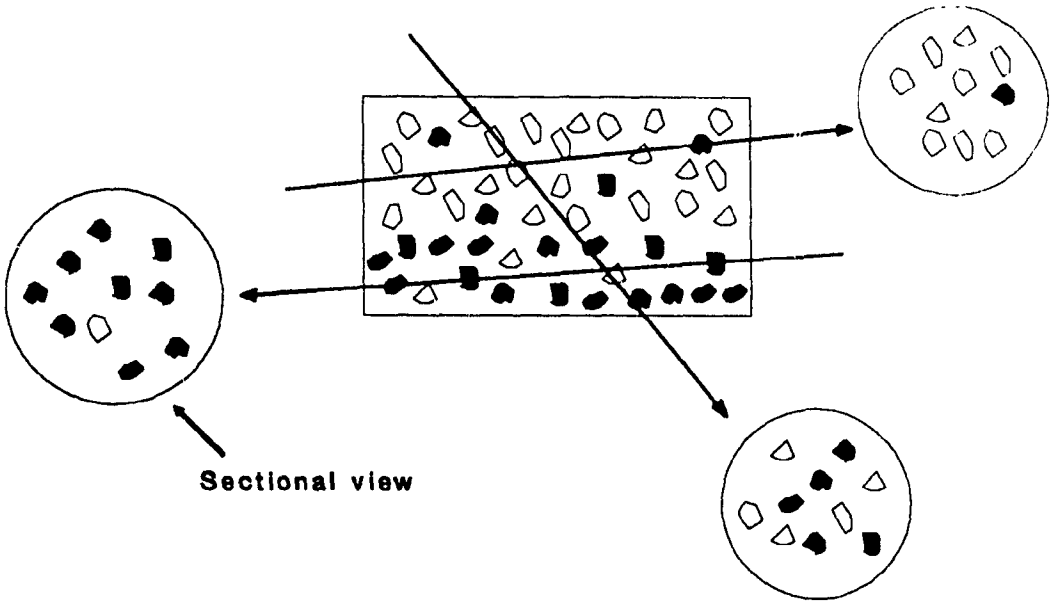

Figure 2.1 : Particle segregation in the mounting medium.

2.2.4 Polishing

After the mineral particles have been mounted, the surface of the sample must be polished with great care. Under-polishing or over-polishing can create problems in the integrity of the microscope image. A flat surface is required for accurate imaging; poor polishing can create undesired relief on the polished surface. This may lead to a distortion of particle shapes or the elimination of some particle features as seen by the image analyzer.

2.3 Electron Microscopy

After the sample has been prepared, a series of images must be acquired. The correct electron microscope settings and the proper image analyzer filtering procedures must be used so that the images are acquired quickly and clearly with little loss of information [9, pp.54-55].

When examining the sample on the scanning electron microscope (SEM) or electron microprobe (MP) (the two types of electron microscopes used in this study), the settings must be set so that all the features of the sample are preserved and sent with as little distortion as possible to the image analyzer. To understand how to do this, it is necessary to explain how these microscopes work. Since the SEM and MP are very similar instruments [12], the term SEM will be used for both.

Operation of an SEM is analogous to the operation of an optical microscope: instead of using a beam of light, the SEM uses a beam of electrons and instead of glass lenses, the SEM uses electromagnets to focus the beam. The SEM electron beam is created by passing a current through a filament (usually tungsten) and heating it to a point where electrons are given off. The electrons are accelerated by an electric field and acquire kinetic energy. When the beam strikes the surface of the sample, this energy is dissipated and this yields several signals that are gathered by various detectors in the specimen chamber.

The different signals emitted by the electron beam-sample collisions from the interaction volume (the volume from which the signals originate) are shown in Figure 2.2. The three main types are :

1) Secondary Electrons. These ejected electrons are low energy, weakly bound electrons. Due to their low energy, they cannot travel far before they are recaptured; therefore, they can only be detected if they have escaped from or near the surface of the sample. Because of this, the secondary electron signal only carries topographic information about the sample.

2) Backscattered Electrons. If a primary electron (an electron from the source beam) strikes the nucleus of a sample atom, an elastic collision may occur. The rebounding electron is termed a backscattered electron. Backscattered electrons have more energy than secondary electrons and can escape from deeper within the sample. Because materials with high atomic

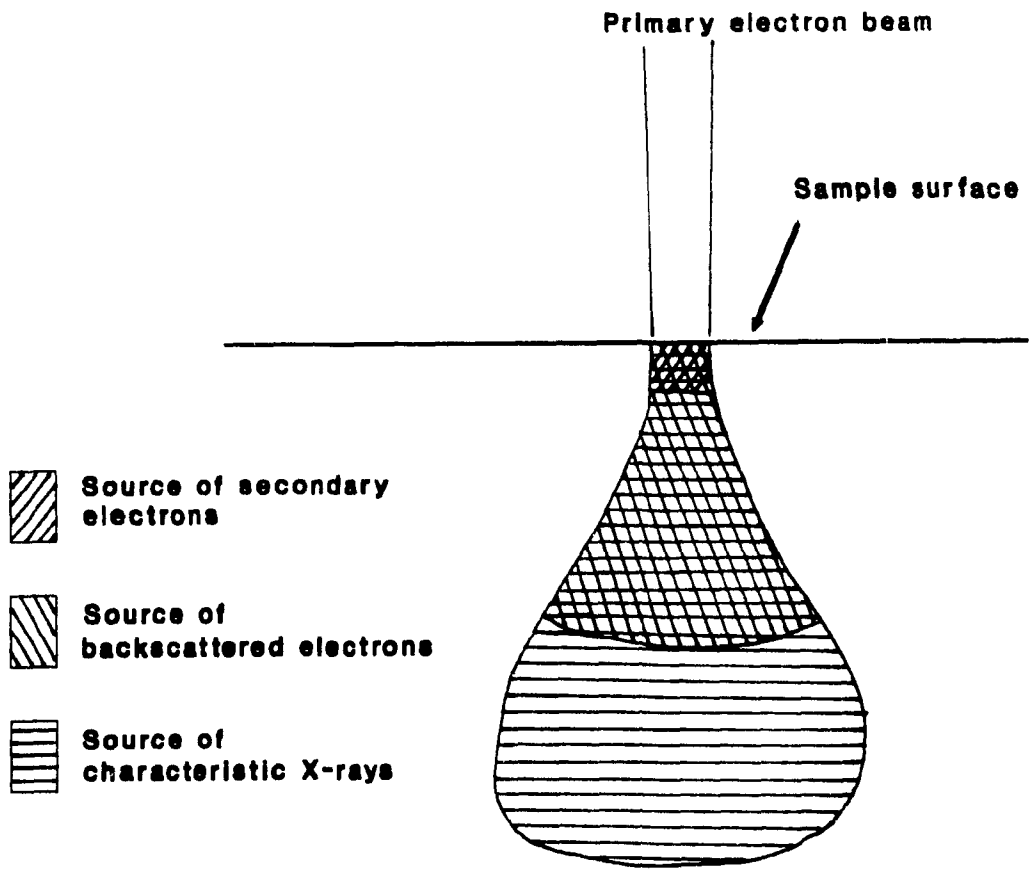

Figure 2.2 : Interaction volume for electron beam - sample collisions.

numbers scatter more electrons than materials with lower atomic numbers, the backscattered signal provides compositional information about the sample.

3) Characteristic X-rays. When a beam electron ejects an inner shell atomic electron from its orbital, outer shell electrons jump in to fill the vacancy. The energy associated with this jump is given off in the form of an X-ray, whose energy is characteristic of the atom from which it came. This type of signal provides elemental information about the sample.

Because a secondary electron image of the sample gives only topographic information and no compositional information, it is of little use for the purpose of liberation analysis except to examine the surface of the sample to see how well the polishing was done. Characteristic X-rays would be useful in a liberation analysis since they yield compositional information, but an X-ray image requires a significant amount of time to generate and has poor resolution (compared to secondary and backscattered images). For the large numbers of particles that have to be analyzed, the acquisition of X-ray images is very time consuming. One system that does use X-ray imaging as well as backscattered imaging is the QEM*SEM system [13].

The backscattered electron image of the sample was the signal used for the liberation analysis in this work. A backscattered image of the sample can be rapidly obtained and it provides the necessary compositional information to

distinguish mineral phases from each other. The different mineral phases appear as different shades of grey. The SEM accelerating voltage, beam current, working distance, contrast and brightness have to be carefully selected to obtain a good backscattered image. SEM controls and their setting in this study are explained below.

1) Accelerating voltage. The accelerating voltage is the potential between the filament (cathode) and the anode which causes the electrons to accelerate. It is usually set at between 10-30 keV. A high accelerating voltage will increase the energy of the primary electrons and produce a large amount of backscattered electrons which in turn will reduce the acquisition time, but a high accelerating voltage reduces the resolution and exacerbates the halo effect (intensity variations that occur around phase boundaries produced by the averaging of the signal in the interaction volume). The voltage was set at 20 keV for these tests.

2) Beam current. The beam current refers to the number of electrons striking the sample per unit time. A large beam current will produce a large amount of backscattered electron emissions, but large beam currents may harm the sample. In these tests, it was set and maintained at 1.5×10^{-8} Amp.

3) Working distance. This term refers to the distance between the sample surface and the final pole piece of the SEM. A short working distance will result in the detection of more backscattered electrons, but the effect of

relief on the signal will increase. It was set here at 30 mm.

4) Magnification. For the purpose of liberation analysis, it has been suggested that the magnification be selected so that the largest particle section diameter is no more than 10% of the image diameter [9, p.49]. This will result in 50-100 particle sections in each image provided the sample contains particles of four or less $\sqrt{2}$ Tyler size classes. If there are too few particle sections per image, the number of images that have to be analyzed is increased. If there are too many particles in each image, then the smaller features of the particles will be below the resolution level and will be impossible to analyze. The magnification was set here at 60x (for 75-106 μm particles) which resulted in about 100 particle sections per image.

5) The brightness and contrast of the image were adjusted so the mineral phases could be easily distinguished.

2.4 Image Analysis

The backscattered image of the polished surface is digitized and sent to an image analyzer for analysis. Image analyzers are computer programs loaded onto a host computer that perform measurements on particle features (such as particle size and liberation distribution) in the image (Figure 2.3). However, before an image analyzer can do any of these measurements, the image from the SEM must first be edited. Halos and grey level variations caused by such factors as relief

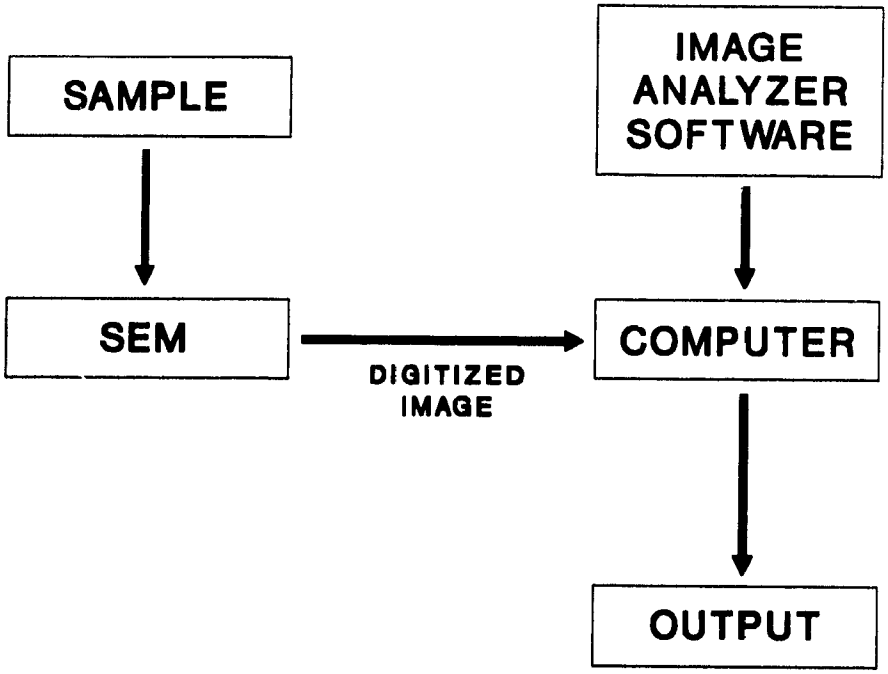

Figure 2.3 : SEM and image analysis.

and subsurface features (i.e. features just below the surface but within the interaction volume) must be removed.

In order to eliminate these variations, the image must be run through a series of filters and enhancement operations. Although these processes 'clean' up the image, they may also alter the image in such a way that particle features are distorted, eliminated or misidentified. For instance, in liberation analyses, some common problems are :

1) Separation of touching particles. It is important that touching particles (two separate particles whose sections are in contact with each other) be distinguished from locked particles. If the filter used to separate touching particles is too coarse, locked particles may accidentally be separated and artifact free sections may be observed. (A partial solution to this problem is presented in Section 5.2.)

2) False mineral phase occurrences. Halos and grey level variations may be misinterpreted by the image analyzer as new mineral phases.

3) Particle shape and size distortion. If the filters employ an erosion and dilation algorithm, this may cause changes in the particle section shape and size resulting in inaccurate measurements.

Care must be taken to avoid these types of problems in the filtering process. Image analysis settings for a typical liberation analysis are explained below.

1) Acquisition time. This refers to the time that is spent digitizing the SEM image. A long acquisition time provides a more accurate image.

2) Frame averaging. If multiple images are digitized from the same SEM image, then they can be averaged together to form a single final image.

3) Grey image filters. These filters are used on the primary grey image (the unaltered image obtained from the SEM) to eliminate halos and to sharpen grain boundaries [14].

4) Selection of grey level envelopes. The correct grey level for each mineral phase must be chosen so that the binary image of each different phase can be produced. Each binary image should include all occurrences of the phase in question and only occurrences of that phase.

5) Binary filtering. The binary images have to be processed to remove small false mineral phase occurrences.

6) Particle separation routine. A structural feature algorithm has to be used to distinguish between touching particles and locked particles [15].

7) Minimum particle section area. The particle section area size below which analysis is not to be performed has to be defined. If a section is smaller than this size, it should not be analyzed due to the fact that small features on these small sections will not be accurately discriminated [9, p.49].

The image analysis procedure used in this work is outlined in Section 5.3.

2.5 Statistical Considerations

For the purpose of statistical validity, up to 10 000 particle sections may have to be examined [9, pp.84-87]. If there are 50-100 particle sections per image then about 100-200 images have to be analyzed. In addition, since liberation analyses are usually done on a size by size basis, several samples have to be analyzed to complete the picture of the liberation distribution of a certain mineral stream. This places constraints on two variables: particle size and analysis time.

1) Particle size. The size of the particles in the sample affects the number of sections seen in the polished surface. If the particle size is large, then there will be fewer particle sections seen per polished surface. If this is the case, then several polished surfaces may have to be prepared in order to arrive at a statistically valid liberation result because some electron microscopes limit the size of the sample that can be placed on their stage. For the purposes of this microscopic liberation analysis, only particles that are in the size range 38 to 106 μm (-150 +400 mesh) will be considered.

2) Analysis time. The accuracy of the digital image is a function of the acquisition time. The image analyzer also requires time to process each image. Since thousands of particle sections have to be analyzed, analyzing one sample can take several hours. Due to the cost of SEM time and the

fact that the number of particles is set (in order obtain a statistically valid result), it is necessary in some cases to compromise between the acquisition and analysis times.

3. STEREOLOGY

3.1 Stereological Effect

There is an inherent error in the measurement of liberation by microscopic examination of a polished surface. The received data comes from a two-dimensional surface while the variable of interest, liberation, is three-dimensional. As a result, there is a bias in the liberation measurements. The degree of liberation will always be overestimated. This type of error will occur regardless of the accuracy of the microscope or the image analysis procedure.

The best method of illustrating this error is by example (Figure 3.1). Free particles will always yield free sections, regardless of the direction of the sectional view, but locked particle can yield either locked or free sections. This will create a situation where there will be artifact free sections seen on the polished surface which will result in an overestimation of free particles. Henceforth, this problem will be referred to as the stereological effect.

3.2 Stereological Correction Methods

Many different methods have been proposed to deal with the stereological effect. Most attempts to correct this problem have tried to derive a

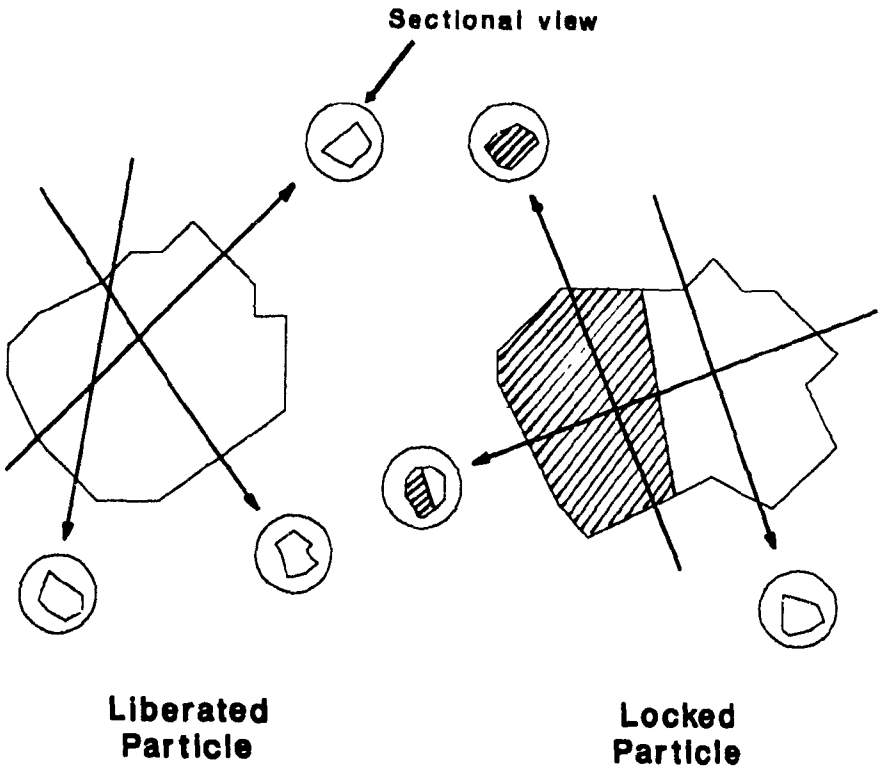

Figure 3.1 : The stereological effect.

transformation matrix such that :

$$\begin{bmatrix}\text{UNCORRECTED}\\ \text{LIBERATION}\end{bmatrix} \times \begin{bmatrix}\text{TRANSFORMATION}\\ \text{MATRIX}\end{bmatrix} = \begin{bmatrix}\text{CORRECTED}\\ \text{LIBERATION}\end{bmatrix} \qquad (3.1)$$

where the uncorrected liberation is the raw data from the image analyzer and the corrected liberation is the estimation of the true liberation distribution of the sample. Efforts to find the transformation matrix have included :

1) simple geometry

2) computer modelling

3) stochastic geometry.

Due to the mathematical complexity of these methods, only a general outline of each is given below.

3.2.1 Simple Geometry

Gaudin [2] and Jones and Horton [16] used simple geometric shapes to represent particles in order to arrive at their transformation matrices. Gaudin is generally thought to have arrived at his 'locking factor' by analyzing a two-phase particulate system of :

1) identically sized spherical particles with

2) a single planar interface between the two phases in the composite particles and with

3) all composite particles having the same grade.

Jones and Horton used Monte Carlo computer simulation to generate linear probes through particles to obtain linear grades. These particles were cubical or spherical with a single interface between two phases.

In both studies, the resulting observed liberation distribution from the sectioning of a series of particles of known composition was recorded. Using this information, a correction model was constructed. Unfortunately, it is difficult to extend the results of these simple geometries to real systems.

An interesting variation on the idea of stereological correction with simple geometry was introduced by Hill [9, pp.172-173] and Hill et al. [17]. They suggested that, rather than defining the transformation matrix for a particular situation, the correction involve determining the boundary values within which the true liberation distribution lies. One boundary was the uncorrected sectioning data, which overestimates the amount of liberation; the other boundary was that obtained by applying the transformation matrix derived for simple locked spherical particles with planar interfaces which gives the worst stereological effect (i.e. it over-corrects the data and underestimates the amount of liberation). The true liberation distribution would lie somewhere between these two extremes. This

method was used on the data of one of the liberation analyses of the standard material in this work.

Hill [9, pp.165-170] further suggested that a simplified correction can be made based on analysis of the results from the sphere model. He found that the locked section distribution more or less accurately represents the true distribution of locked particles. Thus, the problem is reduced to the elimination of free sections originating from locked particles (i.e. artifact free sections). This was accomplished by sectioning the spheres at different grades and arriving at a matrix that gives the amount of artifact free sections produced by different particle grades.

3.2.2 Computer Modelling

This approach involves extensive computer modelling and simulation to arrive with a discretized general transformation function. In one approach, irregularly shaped particles are generated and randomly sectioned by computer [18]. The observed liberation distribution for different particle compositions was recorded. This resulted in a general transformation function that varies according to dispersion density (number of grains per particle), the average volumetric grade and the particle shape. Some subjective textural characterization of the ore is required in this approach.

3.2.3 Stochastic Geometry

Barbery [19] attempted to correct linear liberation data by reconstructing the particles in three dimensions by applying stochastic techniques (the use of random variable sets in a nondeterministic system) to the two dimensional textural information of the particle sections.

Unfortunately, the effectiveness of some of these methods has yet to be determined. These methods offer a corrected result, but since the true result was never known, the accuracy of the corrected result is not known. Because of this, it seems reasonable to suggest that a standard material is required to test the effectiveness of the correction methods. Since the composition and liberation distribution of a standard material would be known, the corrected result from a stereological correction method can be compared with the true result and thus the accuracy of the correction can be assessed.

There have been attempts to employ a standard material. Miller and Lin [20] have performed depth profile measurements to determine the true liberation distribution of particles of copper and iron ore. They progressively sectioned these particles with parallel planes at regular depth intervals and measured the areal composition at each depth in order to reconstruct the volumetric composition of the particle. The results were compared to stereological corrections based on computer modelling.

Barbery [21] used samples of iron ore consisting of hematite and quartz as a standard material. The samples were fractionated with heavy liquids in order to determine their liberation distribution. The liberation analysis results of this material were compared to his stochastic geometry stereological correction. A book by Barbery soon to be published will reveal the successfulness of the correction procedure.

4. THE STANDARD MATERIAL

4.1 Definition

The standard material of interest here is a two-phase (i.e. binary) material comprising free and simple locked particles of known composition and liberation distribution.

A two-phase standard material is all that is required because liberation is measured for one mineral phase at a time. While the liberation of one mineral phase is being measured, the rest of the mineral phases in the sample can simply be grouped together as the 'second' mineral phase.

It is preferable that the standard material have simple locking (locking such that there is only one interface between the phases). Simple locking is probably the most important of all locking types following the argument that since comminution is aimed at liberation, the mineral which 'misses' liberation will most likely be concentrated in the next simplest class - the simple locked particle class. Simple locking also creates the most severe stereological effect and is, therefore, the best test of any correction procedure.

With knowledge of the composition and liberation distribution of the standard material, it can be used as a check on the effectiveness of different stereological correction methods provided the other components of liberation

analysis (sample preparation and image analysis) are done correctly. We can compare the known liberation distribution with that deduced from section data. A standard, in more general terms, would enable the whole procedure (not just stereological correction) to be tested, although admittedly the source of any error may be difficult to isolate.

4.2 Production Procedure Outline

There have been efforts to use a naturally occurring standard material, but such a material has proven difficult to find because of the strict requirements (i.e. two-phase, simple locking). This work deals with the creation of an artificial standard material. This allows the manipulation of the parameters in the creation of the locked particles (i.e. particle size, grain size, material, etc.) so that the type of locking can be controlled.

The production procedure for locked particles is summarized in Figure 4.1. The proposal is to create the standard material by embedding monosize grains of one phase into a matrix which will act as the second phase. Blocks of this material will be crushed, hopefully fracturing randomly, producing locked and free particles. These particles will be screened into their different size classes and their liberation distribution will be determined by an incremental heavy liquid fractionation. By determining the densities of the particles, it is a simple task to calculate the composition and thus the liberation distribution of the particles since

1. Embedding of monosize grains into a matrix.

2. Grinding the grain-matrix blocks.

3. Size classification of the particles.

4. Density classification with a heavy liquid.

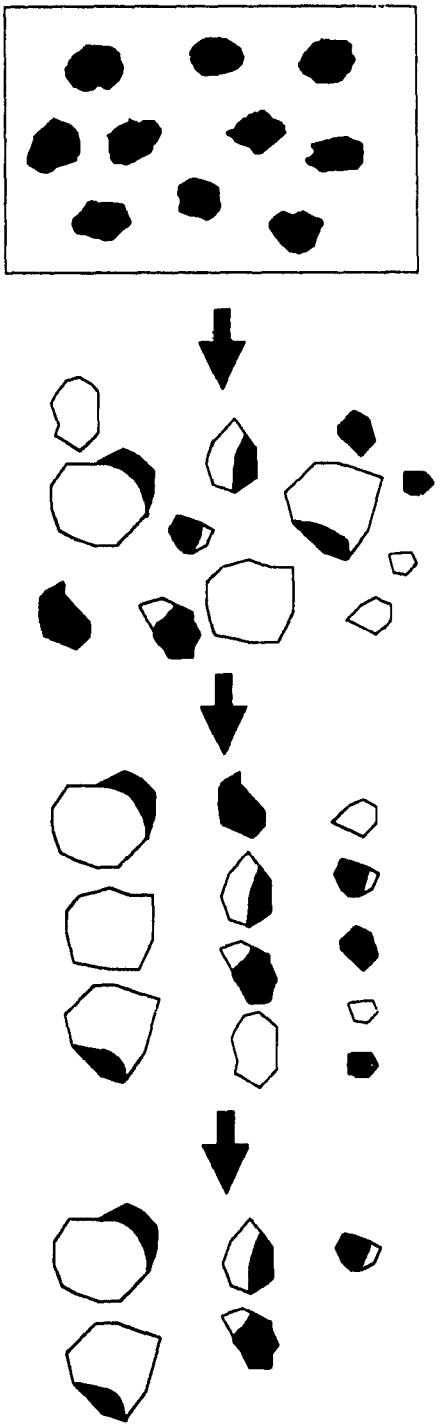

Figure 4.1 : Production of locked particles.

the particles are binary and the densities of the two phases are known. The calculation is as follows:

For a locked particle consisting of only two phases (A and B), the density is :

$$\rho_P = \frac{\rho_A V_A + \rho_B V_B}{V_A + V_B} \tag{4.1}$$

where

V_A = volume fraction of phase A in the locked particle

V_B = volume fraction of phase B in the locked particle

ρ_A = density of phase A

ρ_B = density of phase B

ρ_P = density of the locked particle

but

$$V_A + V_B = 1 \tag{4.2}$$

Substituting equation 4.2 into equation 4.1 gives :

$$V_A = \frac{\rho_P - \rho_B}{\rho_A - \rho_B} \tag{4.3}$$

The production method used here is similar to the method used by Bagga [22] to create particles in order to validate liberation models, but the particles created in this work are much finer and offer a complete liberation distribution.

Creating free particles is a trivial matter; the focus of this work will be on

the creation of locked particles. To create locked particles, the two phases must be selected so that :

1) The grain and the matrix material bind well. This is important since breakage along the interface of the two phases (liberation by detachment) would create free particles.

2) The grain and the matrix material are relatively brittle. This will create material that fractures easily. This may also reduce liberation by detachment, because if the two phases fracture with ease, there should be less tendency for breakage along the interfaces.

3) The grain and matrix material have similar fracture properties. This will promote random fracturing.

4) The matrix material does not trap air bubbles and allows easy embeddment of the grain material. If air bubbles are trapped in the matrix material, the density of the matrix will not be homogeneous.

5) There is a significant density difference between the two phases. The heavy liquid separation will be more accurate if the density difference between the two phases is large, but neither phase must have a density greater than the maximum density of the heavy liquid.

In this work, the two phases of the artificial standard material were silica (grain material) and an epoxy resin (matrix material). Silica fractures readily and

although epoxy resin does not, it does bind well with the silica. The fracture properties of the epoxy resin can be increased by submerging the silica/resin blocks in liquid nitrogen prior to crushing. Silica is easily embedded into the epoxy resin and the epoxy resin viscosity is low enough so that air bubbles can be centrifuged out. Epoxy resins with different properties were tried. The approximate density of epoxy resins is 1.2 g/cm^3 while the density of silica is around 2.6 g/cm^3; therefore, a significant density difference exists that can be exploited by heavy liquid separation. The production method is outlined in detail in the next section.

5. EXPERIMENTAL PROCEDURE

5.1 Production of Locked Particles

The procedure for the production of locked particles for a standard material requires four steps :

1) grain material embeddment

2) crushing

3) wet screening

4) heavy liquid fractionation.

Each step is described in detail below.

5.1.1 Grain Material Embeddment

Before the silica is embedded into the resin, the density of the resin and the silica have to be measured in order to determine the density of the free particles (i.e. the true endpoints of the separation). The density of the resin was measured by creating a block of it in a mold and using a water displacement technique. The density of the silica was measured with an air pycnometer.

The embedding procedure was as follows :

1. The silica was screened into the appropriate size class.
2. The resin and its corresponding hardener were mixed together. The ERL-4221 epoxy resin (Union Carbide, Inc.) was created by adding the resin to an equal part by weight Hexahydro-4-methylphthalic anhydride (Aldrich Chemical Company, Inc.) and 1% by weight Benzyldimethylamine (BDMA) (Ladd Research Industries, Inc.).
3. 50 ml plastic centrifuge tubes were each filled halfway with resin.
4. Small incremental quantities of silica were added to these centrifuge tubes and the mixture was stirred manually. After each addition, the tube was centrifuged for two minutes at 2400 rpm so that any air bubbles trapped in the mixture were removed. This was repeated until each of the tubes was nearly filled to the top with resin and silica. The silica should be completely submerged in the resin and there should be no voids in the mixture.
5. The mixture was allowed to sit in the tubes overnight to allow the resin to harden. Since heat was required to aid the polymerization of the ERL-4221, the tubes were placed in an oven at 70 degrees Celsius for 8 hours.
6. After the resin had hardened, the silica/resin blocks were removed from the centrifuge tubes (Figure 5.1).
7. If there was excess resin (resin containing no silica) at the top of the silica/resin block, it was cut off with a band saw.

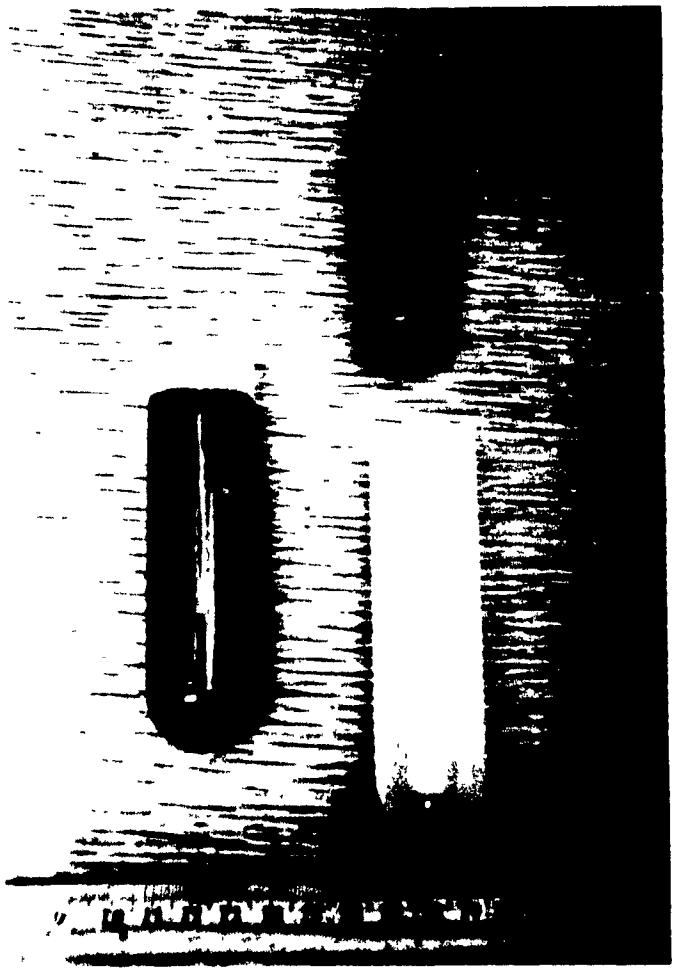

Figure 5.1 : Silica/resin blocks.

5.1.2 Crushing

The procedure for the crushing of the silica/resin blocks was as follows :

1. The silica/resin blocks were submerged in a liquid nitrogen bath to embrittle the resin. After 15 to 20 minutes, the blocks were removed from the liquid nitrogen and broken manually with a hammer into pieces that were smaller than 12 cm^3.
2. These pieces were re-submerged in the liquid nitrogen for another 15 to 20 minutes.
3. Approximately 50 cm^3 of the material was placed in the annular space of the Siebtechnik shatterbox (Figure 5.2) with the puck only (no ring) and crushed for 2 minutes (1 minute for ERL-4221 resin). The shatterbox comminution action is derived from the rapid vibration of the chamber resulting in the trapping and crushing of the material between the puck and wall.
4. The material was removed from the shatterbox and submerged in a small amount of liquid nitrogen.
5. The liquid nitrogen was allowed to evaporate and the material was placed in the shatterbox with the puck and ring and crushed for 2 minutes (1 minute for ERL-4221 resin).
6. In the event that the material did not fit into the shatterbox with the puck

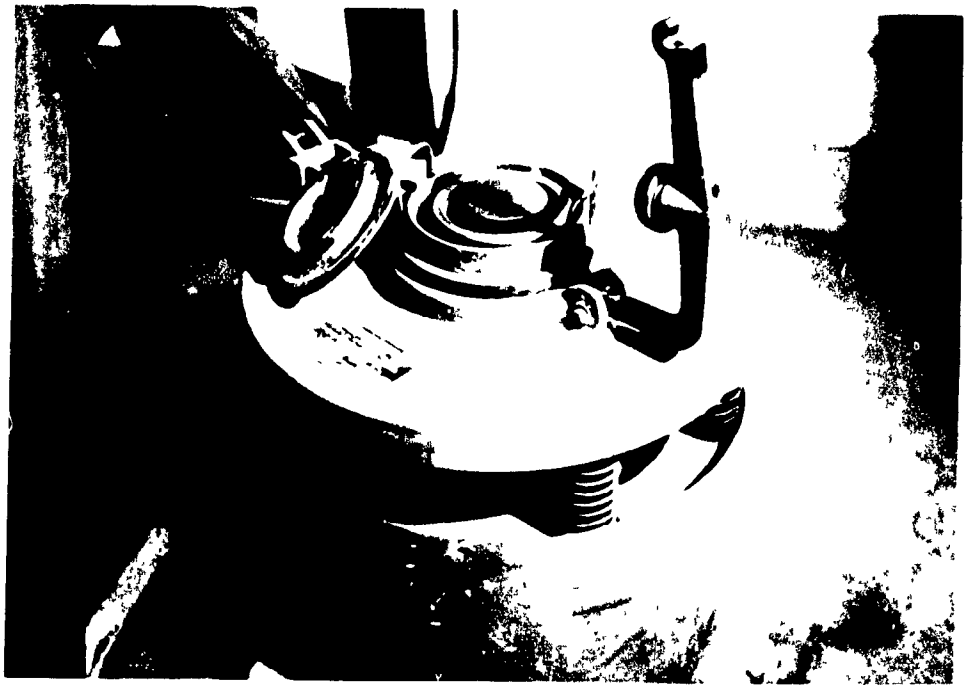

Figure 5.2 : Shatterbox.

and ring, step 3 was repeated.

7. After crushing with the puck and ring had been performed, the material was screened. Material that was greater than 212 μm (65 mesh) was crushed with the puck and ring again. This was repeated until all the material was less than 212 μm.

5.1.3 Wet Screening

The material was size classified by wet screening with the Fritsch wet vibratory sieve shaker (Figure 5.3) (static charge caused the material to adhere to the sides of the screens in dry screening). The screening procedure was as follows:

1. About 100 cm^3 of the material was placed in a beaker and water was added to create a slurry.
2. A few drops of a wetting agent (Triton X-405) was added to the slurry to disperse the particles.
3. The slurry was then placed on the screens in the Fritsch. The Fritsch uses jets of water and a vibratory action on the screens to allow the particles to report to their proper size class. The material was screened for about 15 minutes (at which point, there were no more particles reporting to the undersize stream) at a moderate vibration rate at each screen size.
4. The material was screened into the following size classes :

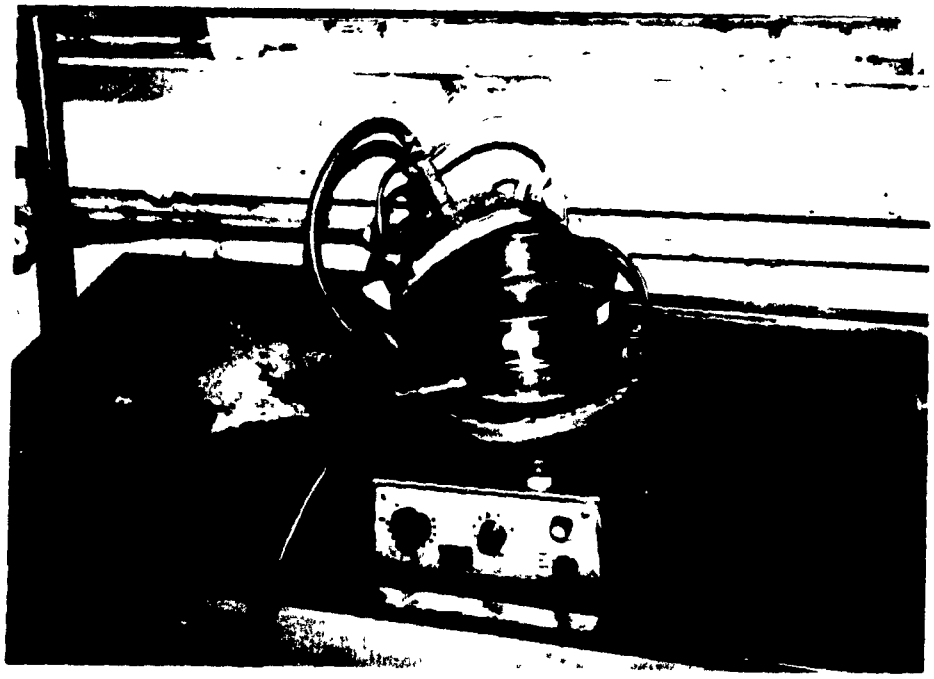

Figure 5.3 : Fritsch wet vibratory sieve shaker.

1) 212 to 106 μm (-65 mesh +150 mesh)

2) 106 to 75 μm (-150 mesh +200 mesh)

3) 75 to 53 μm (-200 mesh +270 mesh)

4) 53 to 38 μm (-270 mesh +400 mesh)

5) less than 38 μm (-400 mesh)

5. All the material was dried in an oven. The temperature of the oven was never allowed to exceeded 100 degrees Celsius (otherwise the resin may start to burn).

6. After the material had dried, it was weighed and the size distribution was recorded.

5.1.4 Heavy Liquid Fractionation

The heavy liquid used in the density separation of the particles was a sodium polytungstate (SPT) solution. SPT ($3Na_2WO_4 \cdot 9WO_3 \cdot H_2O$) is an inorganic salt. SPT powder can be dissolved in water to produce a liquid with a density ranging from 1.0 g/cm^3 to 3.1 g/cm^3. The density of the SPT solution was measured with a 100 ml pycnometer bottle. The density was adjusted by adding water or removing water (by evaporation).

The separations were performed in 125 ml polypropylene separatory funnels. Approximately 100 ml of SPT solution and about 5 grams of the material were

placed in each funnel and each was agitated for 5 minutes so that the particles of the material were completely wetted. In order to prevent particle entrapment (i.e. the misplacement of light particles due to a large number of heavy particles moving quickly downward or vice versa), it is advisable to keep the volume of particles in each funnel to a minimum.

The funnels were centrifuged to accelerate the separation and to break up any flocs of the material. After centrifuging, in the majority of cases, there was a clear interface between the heavies and the solution and the lights and the solution indicating that a precise separation had taken place. In some cases, the solution was cloudy due to the presence of near density particles and backmixing (caused by centrifugal deceleration). To ensure that the separation is as precise as possible, this first separation, a rougher stage, was followed by another separation, a cleaner stage. That is, the heavies and lights from the rougher are individually placed into the SPT solution with the same density as the rougher in order to re-direct the misplaced material. The flowsheet of this process is shown in Figure 5.4.

In the rougher stage, the funnels were centrifuged for 5 minutes at the top centrifuge speed (2380 rpm). In the cleaner stages, the funnels were agitated and then centrifuged at a gradually increasing speed so that the chance of particle entrapment is reduced. The centrifuge speeds and times in the cleaner stages are shown in Table 5.1.

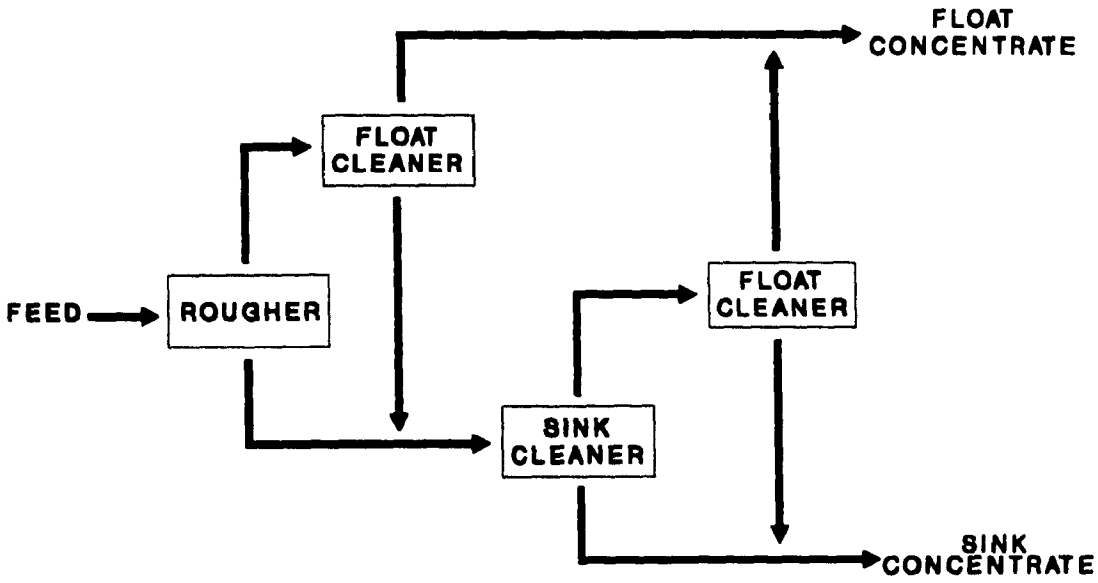

Figure 5.4 : Heavy liquid separation flowsheet.

Time (minutes)	RPM
1	380
1	790
1	1180
1	1590
1	1980
2	2380

Table 5.1 : Centrifuge speeds and times in the cleaner stages.

The liberation distribution of the locked particles can be found by performing an incremental density fractionation. This will reveal not only how the amount of locked material varies with composition, but it will also provide particles of any given composition for analysis.

5.2 Sample Preparation Procedure

In the sample preparation for this work, a diluent (or filler) material was used. The diluent material serves to separate physically the particles in the sample so that the incidence of touching particles is reduced. The diluent material should have approximately the same atomic number as the mounting medium so that it will become nearly invisible when seen by the SEM with backscattered imaging.

The use of large amounts of diluent material will reduce the instances of particle touching, but it will also reduce the number of particle sections seen per image (field of view). As mentioned earlier, this is undesirable. A balance has to be found between the need to maximize the number of particle sections per image and the need to minimize the instances of particle touching. It was suggested by Hill [9, p.22] that the addition of diluent material to the sample particles in a volumetric ratio of 1:1 was a reasonable compromise. This ratio is for natural particle settling and packing only. Since a centrifuge was used in this sample preparation method, more particle packing resulted and a volumetric ratio of 2:1 (diluent material : sample material) was used. Some researchers use ratios of up to 10:1 [13], but this may severely limit the number of sections seen on the polished surface. The diluent material also helps prevent particle segregation in the mounting medium by hindering the settling and supporting the particles in space.

The samples of the standard material were prepared using the following procedure :

1) The diluent material was mixed with about 0.3 grams of standard material in the volumetric proportion of 2:1.
2) This mixture was placed in a 32 mm mold and 2 ml of resin (mounting medium) was mixed in.
3) The mold was centrifuged for 5 minutes at 2000 rpm to remove any air

bubbles.

4) Resin was added to fill the mold to the top.

5) The resin was allowed to harden overnight.

6) The sample was polished on a Leco polisher at 240, 400 and 600 grit silicon carbide paper for about 3 minutes at each grit.

7) Following silicon carbide polishing, the sample was diamond polished on a diamond polishing wheel at 6, 3 and 1 μm diamond dust for approximately 10 minutes each.

8) The sample was then placed in an ultrasonic bath of methanol to remove any polishing residue that was trapped on the surface.

9) The polished surface was gold-coated to provide electrical conductivity (a thin film of conductive material such as gold prevents a build up of electrons on the polished surface which would degrade the image [23]).

For the initial tests in this work, the matrix material resin was doped with 10% by weight iodoform powder (CHI_3) to increase its atomic number; the mounting medium resin was not doped. This provided a method of distinguishing the mounting medium from the matrix resin when viewing the sample with the SEM.

In later tests, the mounting medium was doped with iodoform while the matrix resin was not doped. By controlling the doping (and thus the backscattered grey level) of the mounting medium, the image contrast could be adjusted without

having to change or dope the matrix resin.

When the mounting medium was undoped, graphite particles were used as the diluent material. When the mounting medium was doped, particles of hardened and crushed doped resin were used as the diluent material. The curing of the doped resin generated a large quantity of heat and consequently it had to be cured in an ice bath.

5.3 Image Analysis of the Standard Material

The standard material to be analyzed was mounted as described above and a liberation analysis was performed. The results of this liberation analysis were compared with the model prediction of the sectioning of simple locked spheres with planar interfaces. In each sample, the particle size was 75 to 106 μm. The facilities at CANMET were used to perform this analysis. The equipment consisted of a Jeol MP and a Kontron image analyzer. The images were stored in 512x512 pixel image areas. The settings of the MP were as described in Section 2.3. The procedure for image analysis was as follows:

1) The acquisition time was set at 7 seconds per image. Frame averaging was not used since only one image was acquired. This image is referred to as the primary grey image.

2) A grey level filter called DELIN was used on the primary grey image. This

filter helped minimize the halo effect by sharpening particle boundaries by removing grey level variations around particle edges. This filtered image is called the secondary grey image.

3) The primary binary images were created by choosing grey levels that represented the different phases in the secondary grey image. The grey levels for the two phases in this case were easily selected. Since the resin of the standard material had a lower atomic number than the silica, the resin occupied the low (dark) end of the grey level spectrum while the silica occupied the high (bright) end of the spectrum. The mounting medium (which was doped) occupied an intermediate part of the spectrum.

4) The binary processing consisted of four steps :

   a) An erosion filter was used to remove one layer of pixels from each particle section in the primary binary images. One erosion cycle was performed.

   b) A dilation filter was used to add one layer of pixels to each particle section. Two dilation cycles were performed.

   c) This image is ANDed with its primary binary image.

   d) The AFILL filter was used to fill up any small holes in the particles.

This produced a binary image called the secondary binary image.

5) The particle separation algorithm used in this study to separate touching particle sections was as follows :

   a) All the secondary binary images were ANDed together to form a

binary image of all the particles.

b) The particles in this image were eroded for 2 cycles in order to break the contact between touching particles.

c) The particles in this image were identified and then the background was eroded for 4 cycles (the effect is similar to a particle dilation).

d) A boundary around the identified particles was created.

e) The image of the boundary was inverted and ANDed with the binary image of all the particles.

6) The minimum particle section area was selected. As mentioned earlier, small sections should be excluded from the analysis because they may not be accurately discriminated. Another important reason to exclude the smaller sections from the analysis is the fact that smaller sections contain a greater amount of stereological bias [9, p.170]. All sections with areas less than 600 μm^2 were not analyzed [24].

It is important to state the electron microscope and image analysis operation procedure under which the liberation analysis is performed because there is no standard liberation analysis method and different microscope and image analysis operation procedures on the same sample may yield different results.

6. RESULTS AND DISCUSSION

6.1 Preliminary Tests

The first test to produce locked particles was performed with coarse (600 to 850 μm) silica particles (grain material) and a doped Epofix (Struers Inc.) epoxy resin (matrix material). As described in Chapter 5, the silica was embedded in resin, crushed and screened. The resulting size distribution is shown in Appendix A.1.

The density of the silica was measured to be 2.62 g/cm^3 (±0.004 with 4 degrees of freedom) and the density of the doped Epofix resin was 1.22 g/cm^3 (±0.0006 with 4 degrees of freedom). A heavy liquid separation was performed on the 38-75 μm (-200 +400 mesh) particles and the 75-150 μm (-100 +200 mesh) particles at 1.30 and 2.50 g/cm^3, which is equivalent to 5.6 and 91.4 volume % silica, respectively, to remove 'free' silica and 'free' resin.

These two endpoints (5.6 and 91.4 volume % silica) were selected rather than 0 and 100 volume % silica because of the problem of separating near-liberated particles from the large number of completely liberated ones. A separation very near the density of either the resin or the silica yielded poor results. In this work, therefore, material that was less than 5.6 volume % silica was considered to be free resin while material that was greater than 91.4 volume % silica was

considered to be free silica. The material with a composition between these two endpoints was considered to be locked.

Less than 1% of the mass reported as locked particles in this first test, the other 99% being either free silica or free resin. This result probably reflects the fact that there was a relatively small amount of interfacial area between the silica and the resin due to the coarseness of the silica. There was an insufficient amount of material to perform an incremental density fractionation but, nevertheless, the particles were mounted and examined under the SEM. SEM photographs (Figures 6.1 and 6.2) confirmed that locked particles were created. The bright phase in the photographs is the silica, the light grey phase is the doped Epofix resin and the dark grey background is the mounting medium. The faint, textured particles in the mounting medium are the diluent material particles (graphite in this case). Although all the particles in the sample were locked, some free sections can be seen as a result of the stereological effect. A majority of the locked particles exhibited simple locking, but there were some complex locked particles as well. Because the amount of locked material produced was so small, emphasis was placed on increasing the production of locked particles.

6.2 Grain Size Test with Epofix

The most effective method of increasing the amount of locked material would be to decrease the grain size. In Figure 6.3, it can be seen that reducing the

Figure 6.1 : SEM photograph of [600-850 µm grain/38-75 µm particle/doped Epofix] locked particles.

Figure 6.2 : SEM photograph of [600-850 µm grain/75-150 µm particle/doped Epofix] locked particles.

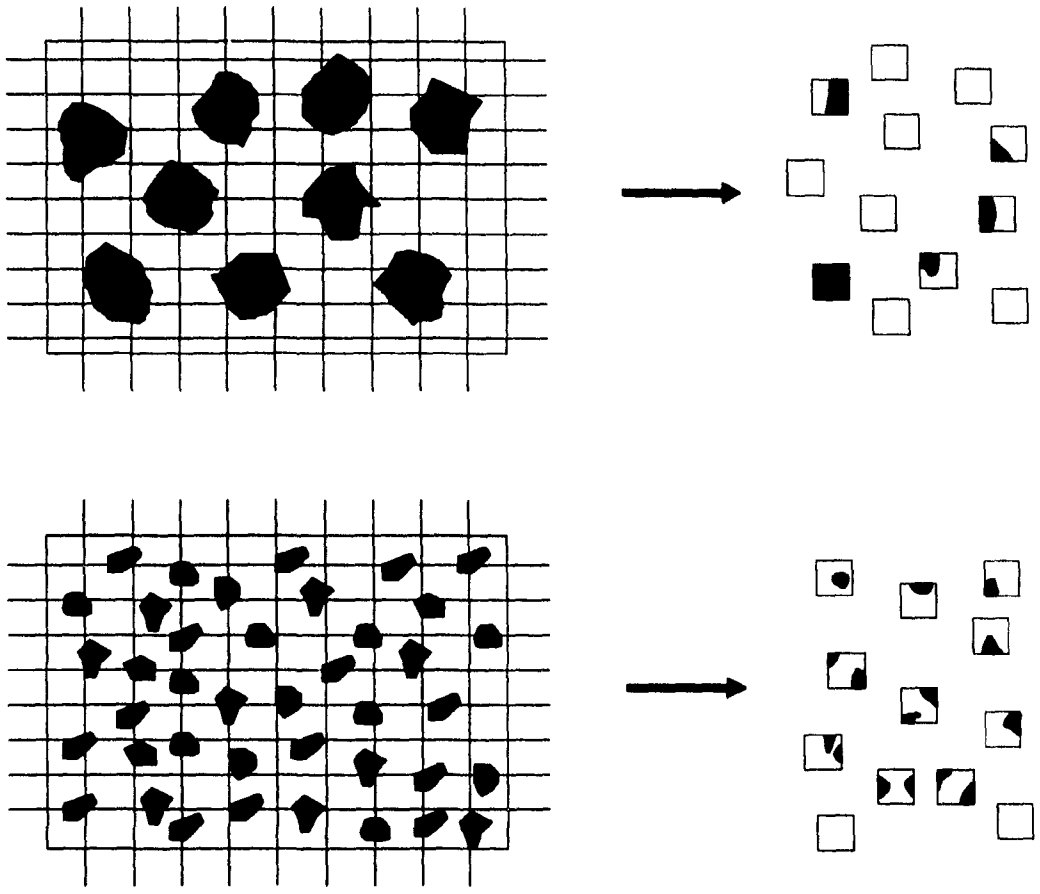

Figure 6.3: Grain size effect on locked particles.

grain size increases the interfacial area between the two phases. This will result in an increase in the probability of forming locked particles. Unfortunately, there is a constraint on decreasing the grain size. If the grain size is much smaller than the particle size (the size of the material after it has been crushed), then the occurrence of complex locking will increase. As mentioned earlier, simple locking is desired for the standard material. A compromise must be found between the amount of locked material produced and the amount of simple locking produced.

The effect of grain size on the amount of locked material produced and on the type of locking was tested using Epofix resin and two different silica sizes. In the first test, 38-53 μm (-270 +400 mesh) silica was used and in the second test 75-106 μm (-150 +200 mesh) silica was used. As before, the material was crushed, screened into different particle size classes (the size distributions are shown in Appendices A.2 and A.3) and a heavy liquid separation was done to remove free silica and free resin. The amount of locked material produced in both tests for each particle size is shown in Tables 6.1 and 6.2.

The amount of locked material produced is stated as a mass percentage. Although it would be preferable to compare the volumetric percentage of the locked material produced (since this is what is measured in sectioning data), the volumetric percentage cannot be determined without determining the liberation distribution of each sample.

In these tests, the actual amount of silica and resin in the silica/resin blocks will vary depending on the silica size. The size of the silica will determine the

Grain Size : 38 - 53 μm Matrix Resin : Epofix			
Particle Size Class (μm)	Free Resin (Mass%)	Locked Material (Mass%)	Free Silica (Mass%)
75 - 106	0.2	99.8	0.0
53 - 75	11.4	88.6	0.0
38 - 53	9.8	32.0	58.2

Table 6.1 : Locked material production with 38-53 μm silica and Epofix.

Grain Size : 75 - 106 μm Matrix Resin : Doped Epofix			
Particle Size Class (μm)	Free Resin (Mass%)	Locked Material (Mass%)	Free Silica (Mass%)
106 - 150	42.6	56.4	1.0
75 - 106	26.4	12.7	60.9
53 - 75	22.5	4.4	73.1
38 - 53	24.2	2.7	73.1

Table 6.2 : Locked material production with 75-106 μm silica and doped Epofix.

size of the void spaces to be filled by the resin. Although the volumetric ratio of silica to resin in the silica/resin blocks will affect the amount and the composition of the locked material, it cannot be independently varied and is set for each test due to the nature of the formation of the blocks (the centrifuge causes the silica to be packed with a packing density that depends on the silica size). It was found that for both 38-53 μm and 75-106 μm silica, the silica/resin blocks were about 50% silica by volume.

Although the tests performed in Table 6.1 used undoped Epofix and Table 6.2 used doped Epofix, the results can be compared because the doping of the resin does not noticeably affect the resin fracturing properties. As expected, when the particle size was greater than the grain size, a large quantity of the material became locked and a small quantity of free material was produced. When the particle size was smaller than the grain size, the amount of locked material was greatly reduced and the amount of free material increased. There appeared to be a sharp decrease in the amount of locked material produced at the point where the grain size was the same as the particle size.

Some samples were created and photographed with the SEM. Figure 6.4 shows locked material where the particle size is larger than the grain size; Figure 6.5 shows locked material where the particle size and the grain size are the same; and Figure 6.6 shows locked material where the particle size is smaller than the grain size.

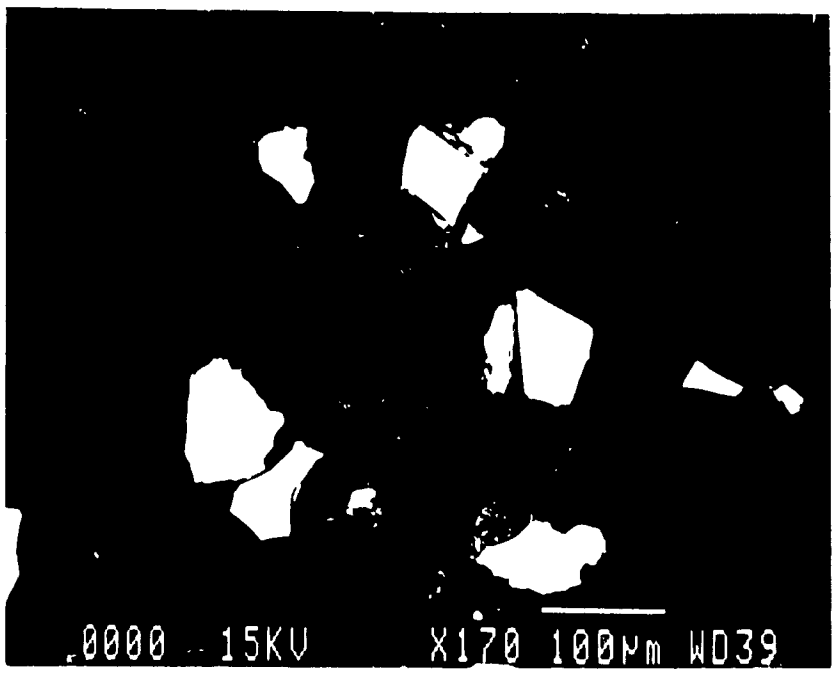

Figure 6.4 : SEM photograph of [75-106 µm grain/106-150 µm particle/doped Epofix] locked particles.

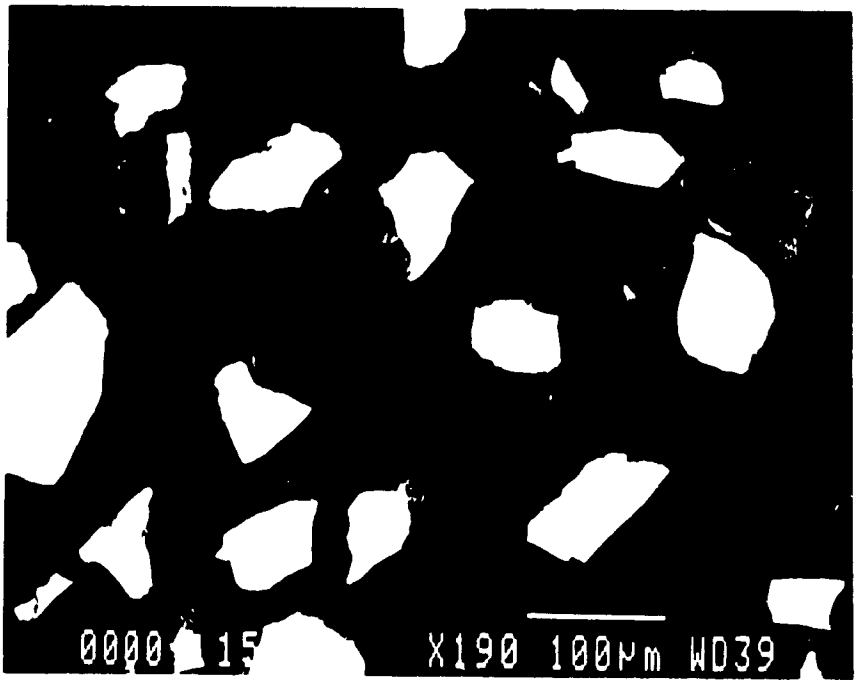

Figure 6.5 : SEM photograph of [75-106 µm grain/75-106 µm particle/doped Epofix] locked particles.

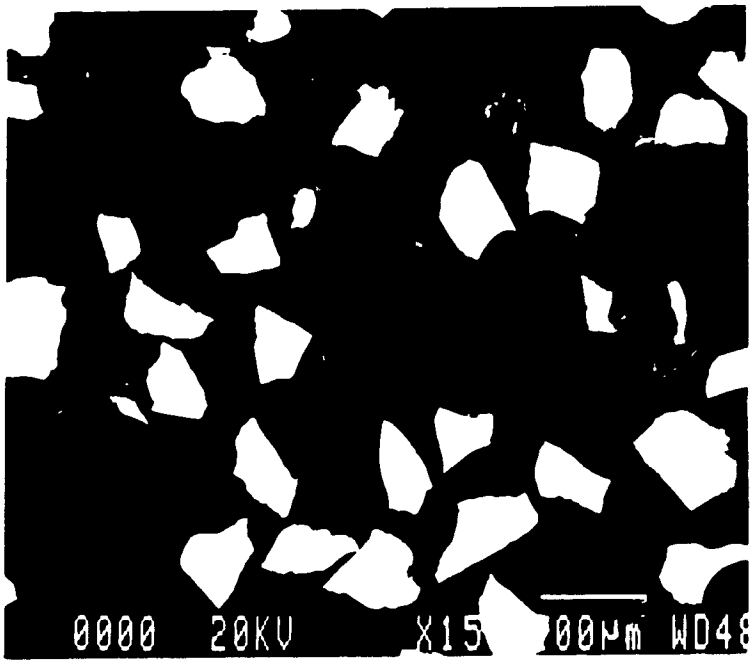

Figure 6.6 : SEM photograph of [75-106 µm grain/53-75 µm particle/doped Epofix] locked particles.

Although a large amount of locked material was produced in the cases where the particle size was larger than the grain size, Figure 6.4 reveals that most of the locking was complex as anticipated. In the case where the particle size was smaller than the grain size, there was a smaller amount of locked material produced, but the particles tended to exhibit simple locking (Figure 6.6). In the case where the particle size and the grain size were the same, there was an intermediate amount of locked material and the particles tended to exhibit simple locking (Figure 6.5), but there was still some complex locking.

Although the SEM photographs are not conclusive evidence that simple locking has been produced (because the stereological effect will influence the observation of the type of locking), it is intuitive that as the particle size decreases while the grain size remains constant, the chance of complex locking reduces.

An incremental density fractionation was done on the [75-106 μm grain/75-106 μm particle/doped Epofix] locked material. The results are shown in Table 6.3 and the liberation distribution curve is plotted in Figure 6.7. The error associated with the heavy liquid separations was calculated as outlined by Adorjan [25] (see Appendix A.6). Most of the locked particles had a composition greater than 50 volume % silica. A possible explanation for this can be found by considering the breakage of the silica/resin blocks in the shatterbox. Although the shatterbox breaks particles mostly by impact, the plasticity of the resin (even after exposure to liquid nitrogen) resists and cushions this shattering force and as a result, the

Grain Size : 75-106 μm
Particle Size : 75-106 μm
Matrix Resin : Doped Epofix

Spec. Grav. Range	Avg. Spec. Grav.	Vol.% Silica Range	Avg. Vol. % Sil.	Mass (g)	Tot. Vol. (cm^3)	Vol. Sil. (cm^3)	Tot. Vol. (%)	Cum. Tot. Vol. (%)
1.30-1.50	1.40	5.6-20.0	12.8	1.04	0.74	0.10	13.80	13.8
1.50-1.70	1.60	20.0-34.2	27.1	0.47	0.29	0.08	5.46	19.25
1.70-1.90	1.80	34.2-48.5	41.4	0.65	0.36	0.15	6.71	25.96
1.90-2.10	2.00	48.5-62.8	55.7	1.78	0.89	0.50	16.53	42.49
2.10-2.30	2.20	62.8-77.1	70.0	2.54	1.15	0.81	21.44	63.94
2.30-2.50	2.40	77.1-91.4	84.3	4.66	1.94	1.64	36.06	100.00
		Total :		11.14	5.38	1.73	100.00	

Volume % Silica in sample : 60.6%

Table 6.3 : Liberation distribution of [75-106 μm grain/75-106 μm particle/doped Epofix] locked particles.

Figure 6.7 : Liberation distribution of [75-106um grain/ 75-106um particle/doped Epofix] locked particles.

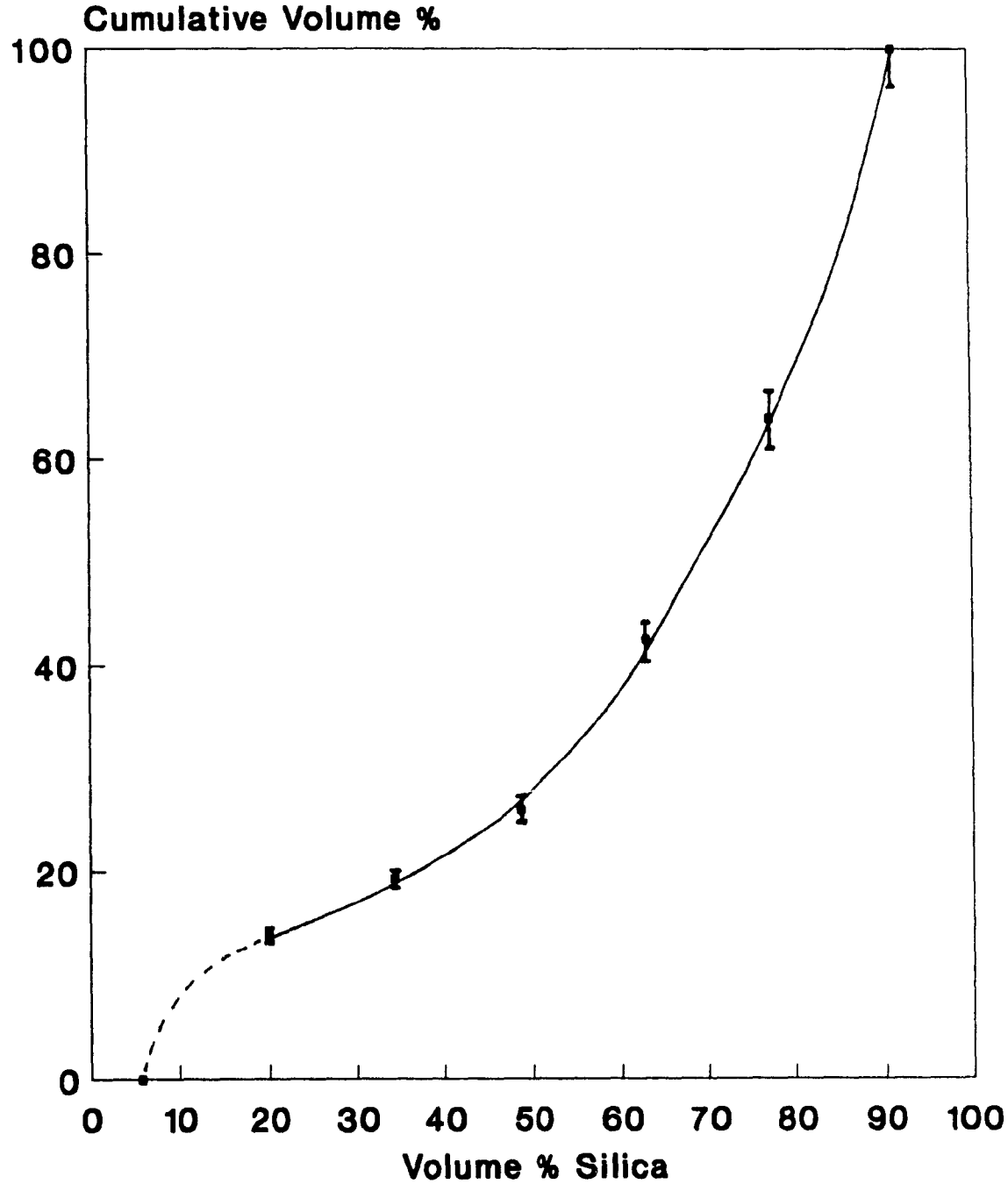

breakage that does occur is caused by abrasion (particularly with finer particles). Since silica is likely to be more abrasion resistant than resin, the resin was preferentially abraded away producing free resin particles and locked particles with a large amount of silica.

With regard to the production of locked material, there were several problems associated with these tests. Firstly, the amount of simple locked particles produced was relatively low. Secondly, the resin used was very difficult to grind due to its plasticity. Thirdly, a close examination of the previous photographs, reveals that there are fine silica particles attached (freckled) to surface of the resin section of the locked particles (Figure 6.8). This last problem could be serious because it may mean the simple locked particles are indeed complex locked particles. All these problems were related to the resin that was used in this test.

Epofix is a resin that is a commonly used mounting medium. Apparently, even when exposed to liquid nitrogen, it does not become brittle and does not break easily. This may account in some part for the production of so few simple locked particles. The freckling of the silica on the resin may be accounted for by two mechanisms :

1) When the silica/resin blocks were ground, fine free silica was formed and during the grinding process, they were embedded into the surface of the resin.

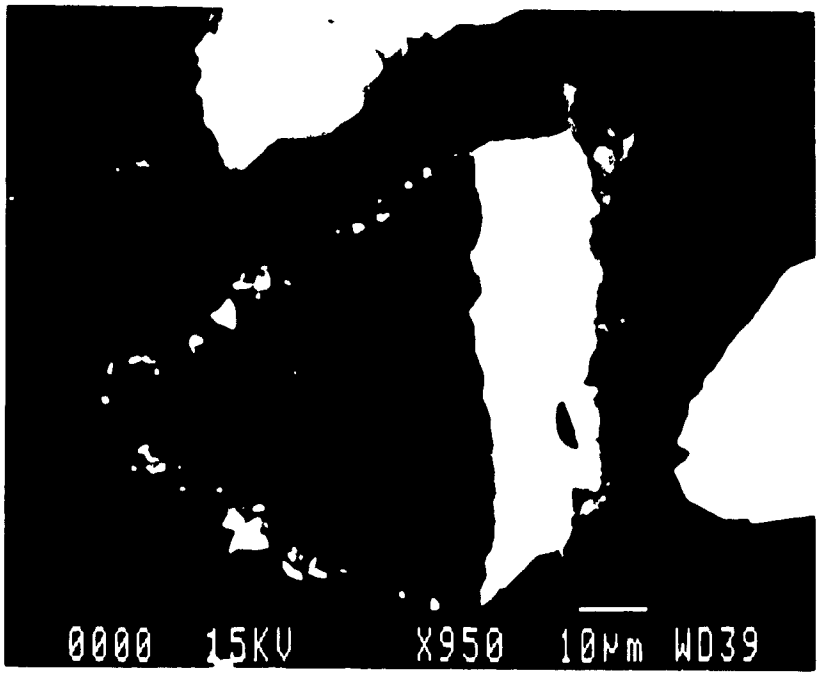

Figure 6.8 : Close-up of [75-106 µm grain/75-106 µm particle/doped Epofix] locked particle showing freckling.

2) The bond between the resin and the silica was very strong and small pieces of silica were pulled off by the resin from silica grains during grinding.

An attempt was made to alleviate this problem by using a different resin.

6.3 Grain Size Test with ERL-4221

ERL-4221 epoxy resin (Union Carbide, Inc.) was selected for testing because it was harder (so embedding of the silica into the resin during grinding would not occur) and more brittle [26] (so allowing easier grinding) than Epofix resin. Its density is 1.21 g/cm^3. Blocks of silica and ERL-4221 were created. The same grain size tests as with Epofix were performed. The size distributions after grinding are shown in Appendices A.4 and A.5. The amount of locked material produced is shown in Tables 6.4 and 6.5.

The same trends as with Epofix were observed. When the particle size was larger than the grain size, a large amount of locked material was produced and when the particle size was smaller than the grain size, a small amount of locked material was produced. Again, a sharp drop in the amount of locked material occurred at the point where particle and grain size were the same. For the case of the 38-53 μm grains, the amount of locked material produced is nearly identical to the corresponding case with Epofix. In the case of the 75-106 μm grains, the amount of locked material produced is significantly higher.

Grain Size : 38 - 53 μm Matrix Resin : ERL-4221			
Particle Size Class (μm)	Free Resin (Mass%)	Locked Material (Mass%)	Free Silica (Mass%)
75 - 106	0.0	98.9	1.1
53 - 75	6.0	88.3	5.7
38 - 53	8.5	30.5	61.0

Table 6.4 : Locked material production with 38-53 μm silica and ERL-4221.

Grain Size : 75 - 106 μm Matrix Resin : ERL-4221			
Particle Size Class (μm)	Free Resin (Mass%)	Locked Material (Mass%)	Free Silica (Mass%)
75 - 106	7.5	32.1	60.4
53 - 75	22.3	11.3	66.5
38 - 53	32.1	6.1	61.8

Table 6.5 : Locked material production with 75-106 μm silica and ERL-4221.

Figure 6.9 shows locked material where the particle size is larger than the grain size, Figure 6.10 shows locked material where the particle size and the grain size are the same and Figure 6.11 shows locked material where the particle size is smaller than the grain size. The bright phase is silica, the dark phase is ERL-4221 and the grey phase is the mounting medium. The faint grey particles in the mounting medium are the diluent material (crushed resin in this case). A close-up of one of the particles (Figure 6.12) of the locked material revealed that the silica freckling problem was greatly reduced.

With both resins, the silica was difficult to polish. Although the polishing was performed under gentle conditions, small pieces at the edge of the silica sections were pulled out; however, this problem was not considered significant enough to affect image analysis.

The [75-106 μm grain/75-106 μm particle/ERL-4221] locked material was selected for liberation analysis. An incremental density fractionation of the locked particles of this material was performed and the results are shown in Table 6.6 and plotted in Figure 6.13 (the error was calculated as outlined by Adorjan [25]). This material was selected because it yielded a relatively high percentage (32.1%) of locked material with an adequate (as judged visually) amount of simple locking. This material was chosen over the [38-53 μm grain/38-53 μm particle/ERL-4221] locked material since larger particles are easier to separate by heavy liquid, easier to mount and polish, and not affected as much by the halo effect. The results of the liberation analysis are described below.

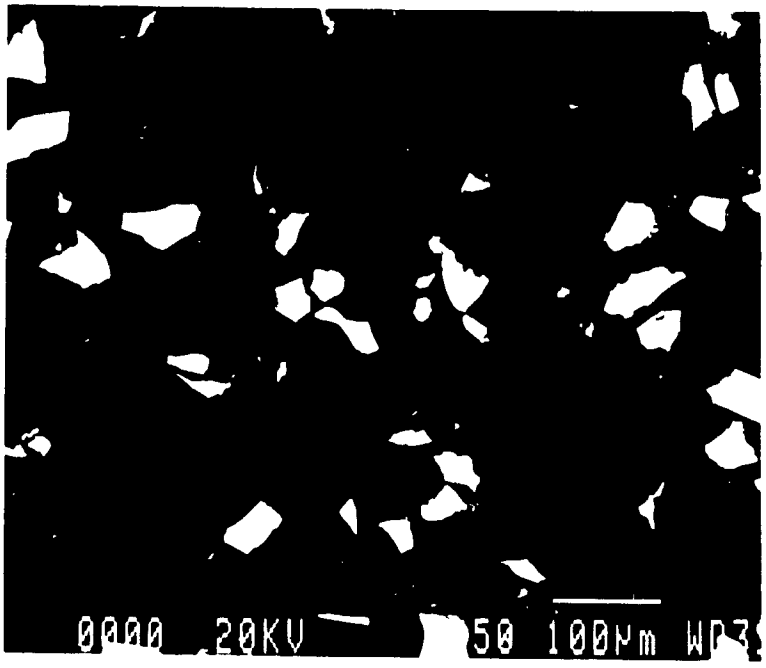

Figure 6.9 : SEM photograph of [38-53 µm grain/53-75 µm particle/ERL-4221] locked particles.

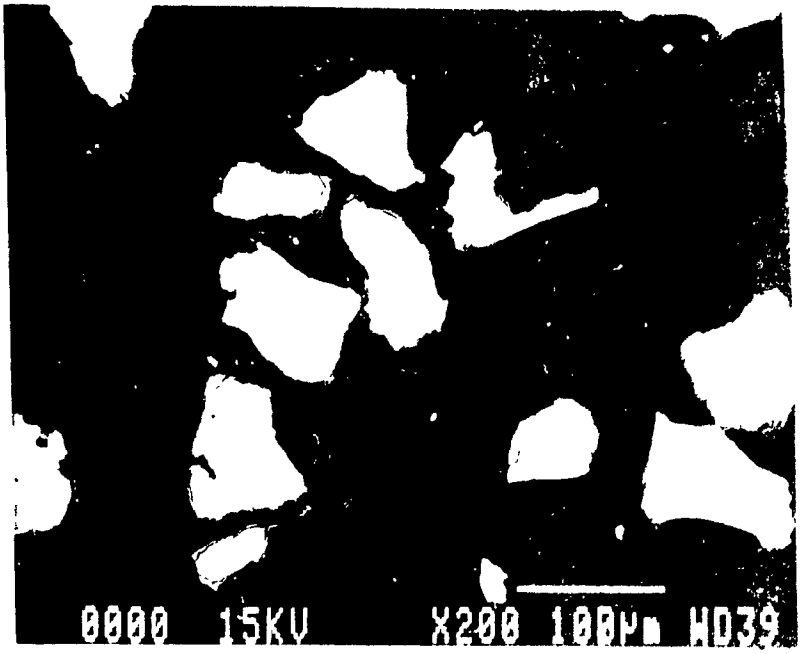

Figure 6.10 : SEM photograph of [75-106 µm grain/75-106 µm particle/ERL-4221] locked particles.

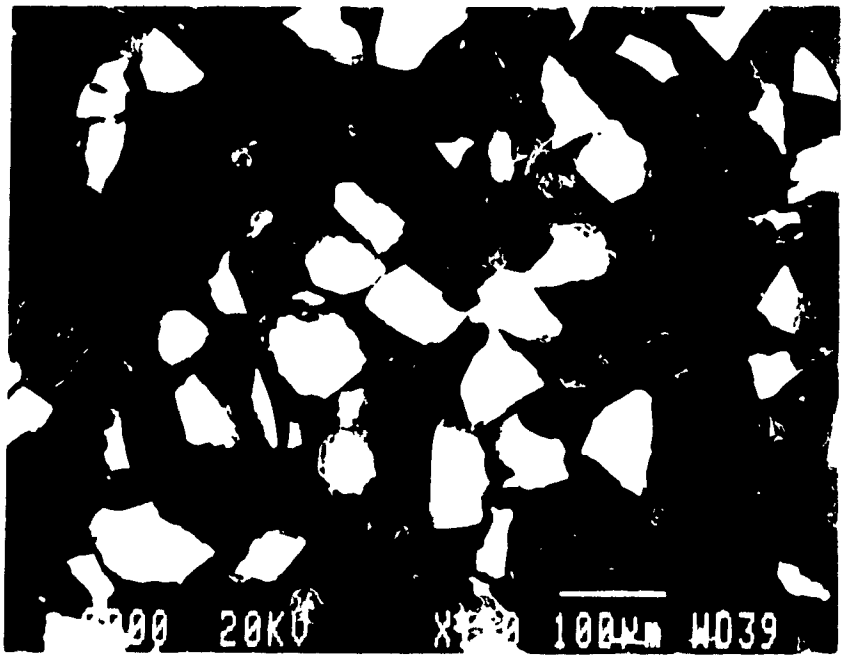

Figure 6.11 : SEM photograph of [75-106 µm grain/53-75 µm particle/ERL-4221] locked particles.

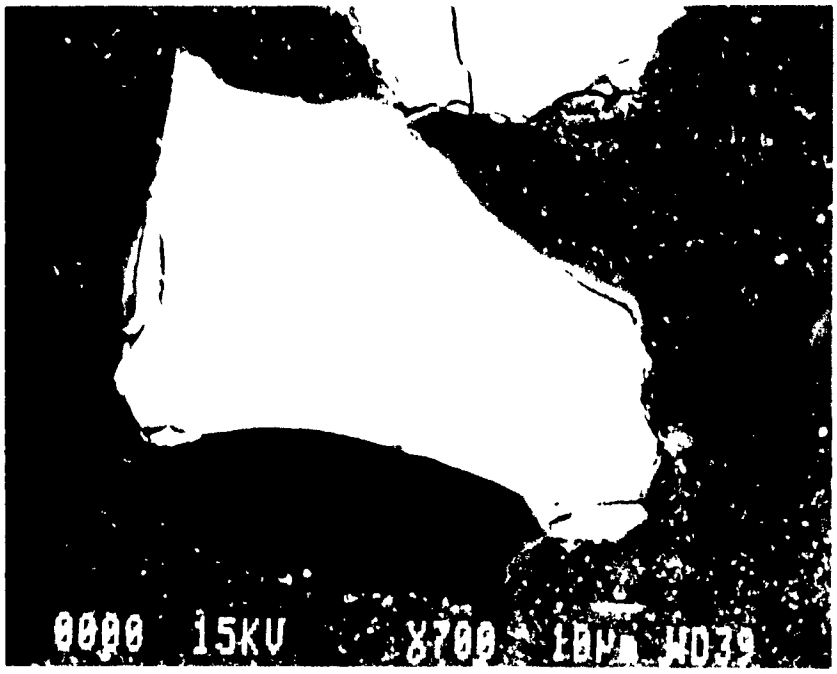

Figure 6.12 : Close-up of [75-106 µm grain/75-106 µm particle/ERL-4221] locked particle.

Grain Size : 75-106 μm
Particle Size : 75-106 μm
Matrix Resin : ERL-4221

Spec. Grav. Range	Avg. Spec. Grav.	Vol.% Silica Range	Avg. Vol. % Sil.	Mass (g)	Tot. Vol. (cm^3)	Vol. Sil. (cm^3)	Tot. Vol. (%)	Cum. Tot. Vol (%)
1.29-1.42	1.36	5.6-15.0	10.3	0.21	0.15	0.02	5.63	5.63
1.42-1.56	1.49	15.0-25.0	20.0	0.14	0.09	0.02	3.11	9.05
1.56-1.70	1.63	25.0-35.0	30.0	0.17	0.10	0.03	3.79	12.83
1.70-1.84	1.77	35.0-45.0	40.0	0.33	0.19	0.07	6.76	19.60
1.84-1.99	1.92	45.0-55.0	50.0	0.53	0.28	0.14	10.06	29.66
1.99-2.13	2.06	55.0-65.0	60.0	0.80	0.39	0.23	14.15	43.81
2.13-2.27	2.20	65.0-75.0	70.0	1.10	0.50	0.35	18.21	62.02
2.27-2.41	2.34	75.0-85.0	80.0	1.47	0.63	0.50	22.86	84.88
2.41-2.50	2.45	85.0-91.4	88.2	1.02	0.42	0.37	15.12	100.00
		Total :		5.77	2.75	1.73	100.00	
Volume % Silica in sample : 62.9%								

Table 6.6 : Liberation distribution of [75-106 μm grain/75-106 μm particle/ERL-4221] locked particles.

Figure 6.13 : Liberation distribution of [75-106um grain/ 75-106um particle/ERL-4221] locked particles.

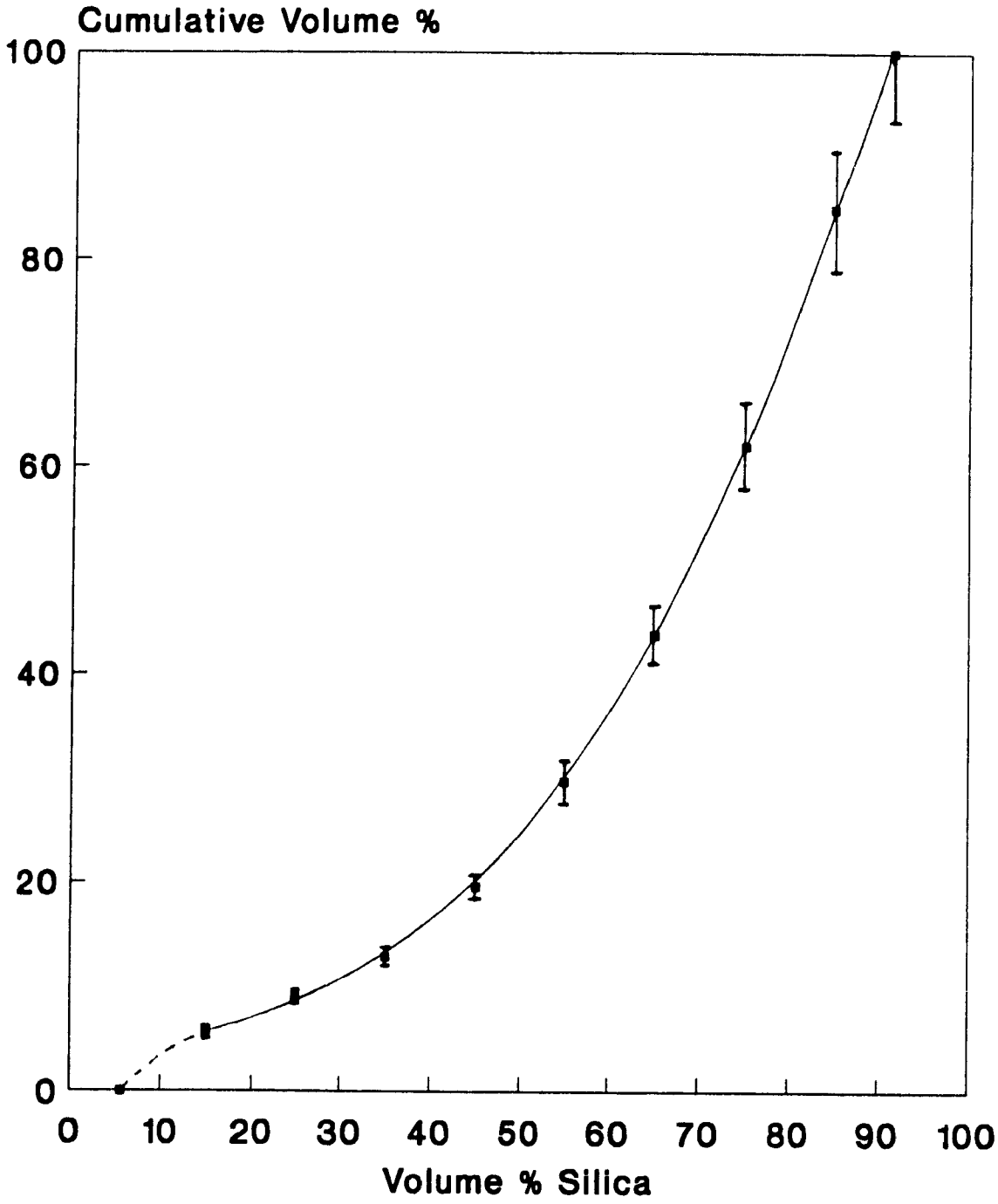

6.4 Comparison with Model Predictions

A liberation analysis was performed on some of the standard material that was created and the results compared to a model prediction. In these tests, [75-106 μm grain/75-106 μm particle/ERL-4221] locked material was used. Three samples were selected from this material. The first sample consisted of particles 45-55 volume % silica, the second sample of particles 75-85 volume % silica and the third sample of particles with the natural liberation distribution of the sample (i.e. it had the liberation distribution shown in Figure 6.13). The image analyzer settings were as described in Section 5.3. Approximately 5000 sections of each sample were examined. The calculation of the statistical error associated with each analysis is explained in Appendix B.1.

Figures 6.14 and 6.15 show the liberation analysis results of the 45-55 and the 75-85 volume % silica material plotted along with the model prediction [9, p.163]. The model prediction is that of the sectioning of a sphere of similar volumetric composition with simple locking and a planar interface. The statistical error (95% confidence interval) associated with the liberation analyses is also given; this error only considers the error due to the number of sections analyzed (i.e. there is no quantification of any systematic error). The liberation analysis data is given in Appendices B.2 and B.3. The model prediction of sphere sectioning is given in Appendix B.4.

Figure 6.14 : Comparison of standard material liberation analysis with model prediction based on the sectioning of 50 vol. % sphere.

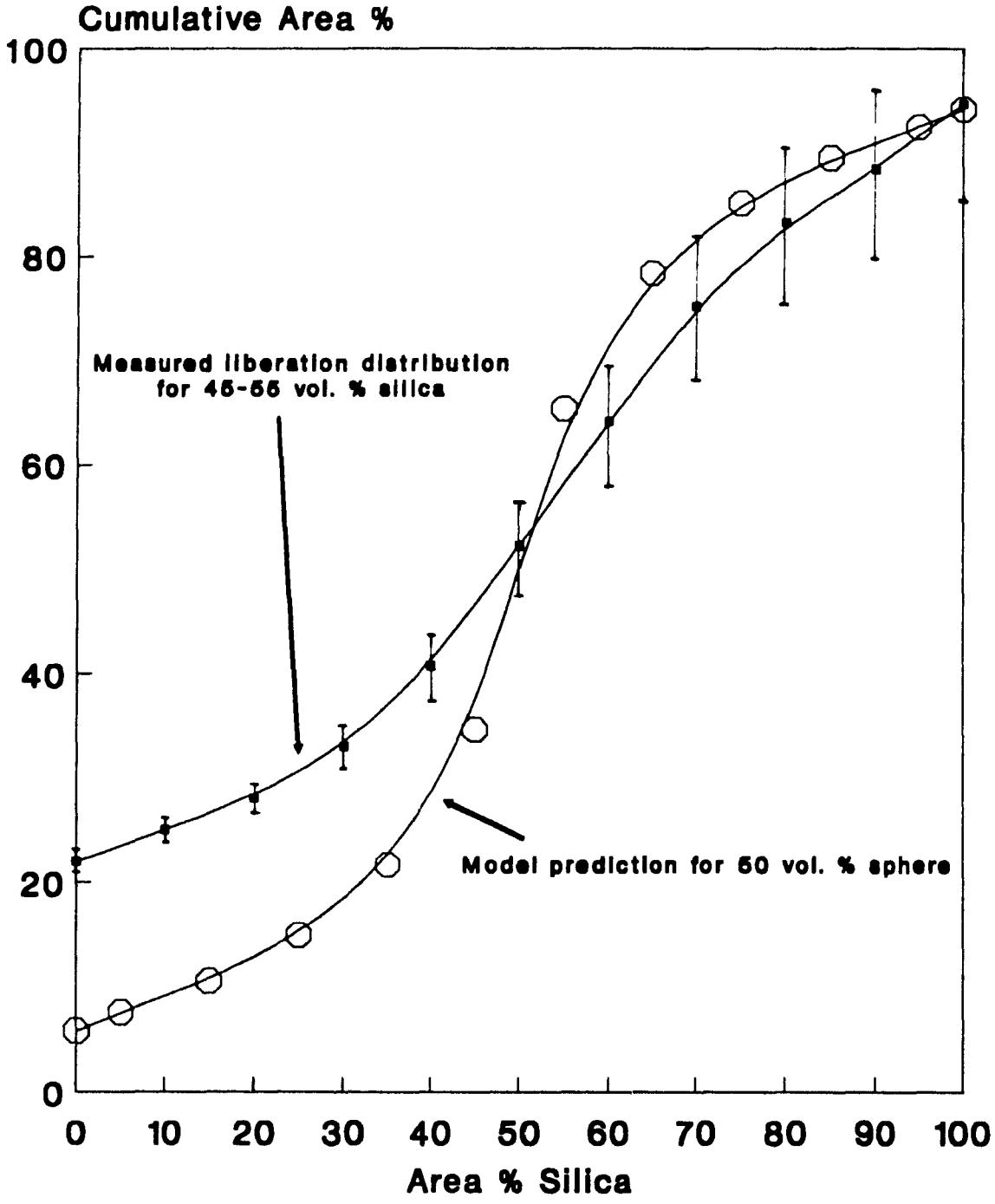

Figure 6.15: Comparison of standard material liberation analysis with model prediction based on the sectioning of 80 vol. % sphere.

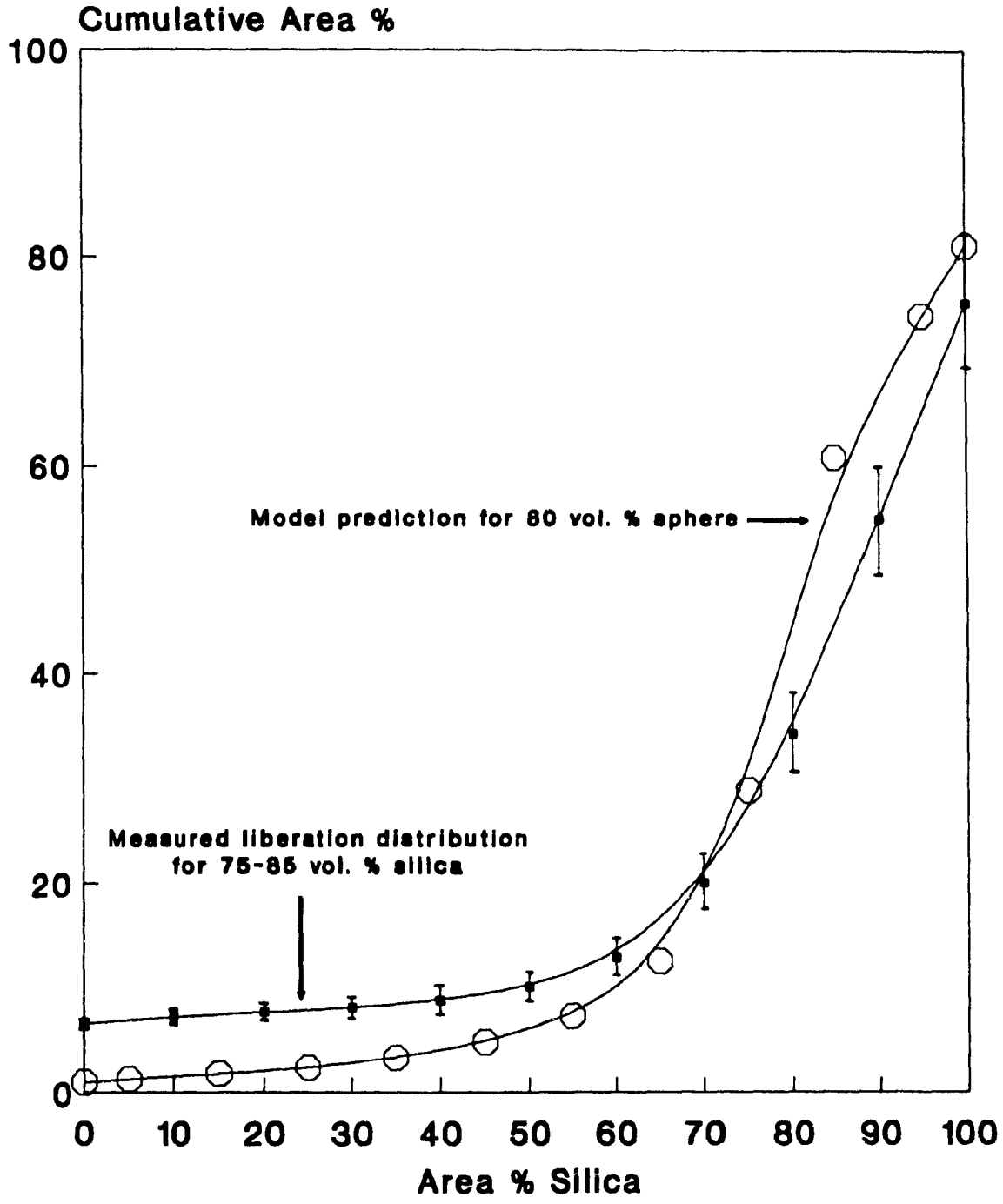

Figure 6.15 shows that the 75-85 volume % silica liberation distribution follows the model prediction for the 80 volume % sphere reasonably well. In Figure 6.14, it can be seen that the liberation distribution of the 45-55 volume % silica does not match the model prediction of the 50 volume % sphere as closely; in particular, the observed sections with a high amount of resin (i.e. low amount of silica) significantly exceeded the model prediction.

The assay of the samples as calculated by the image analyzer should match the measured assay [27] (in this case, the assay given by the heavy liquid separation fractions) and this equivalence is usually used as a criterion of the accuracy of the liberation analysis. For the case of the 45-55 volume % silica material, the image analysis assay was 45.3 volume % silica; for the case of the 75-85 volume % silica material, the image analysis assay was 79.8 volume % silica. The image analysis assay of the 45-55 volume % silica material showed that more resin was detected than actually existed in the sample.

Possible explanations for the discrepancies that occurred in these two cases include :

1) It was difficult to distinguish the matrix resin from the mounting medium resin. Apparently, the backscattered contrast between the two was not sufficient to make a precise identification. In the present case, some of the mounting medium was mistaken to be matrix resin creating an apparent increase in the amount of resin observations (it is understood that the error

could equally well have been to underestimate the matrix resin). This probably caused the single greatest discrepancy between the experimental results and the model predictions. This problem can be remedied by increasing the doping of the mounting medium.

2) The standard material would not exactly follow the sphere sectioning results because the standard material particles were not spherical with simple locking and planar interfaces between the phases.

3) The composition of the particles of the standard material were defined by a 10% range. The average particle composition in this range may not be the same as the composition of the model sphere to which it was compared.

4) Because the effectiveness of the sample preparation method could not be determined, a sample preparation bias could have contributed to the discrepancy [24].

Figure 6.16 compares the results of the image analysis liberation distribution for the particles of the natural liberation distribution with the actual liberation distribution (determined by heavy liquid separation). Also shown is the corrected distribution based on the sphere sectioning model (Appendix B.5). All the data is tabulated in Appendix B.6. The error bars on the observed liberation distribution indicate the statistical error associated with the analysis. The error bars on the actual liberation distribution indicate the error associated with heavy liquid separations. Figure 6.17 shows the same data, but in the form of grade-

Figure 6.16 : Comparison of actual liberation with observed liberation and model correction.

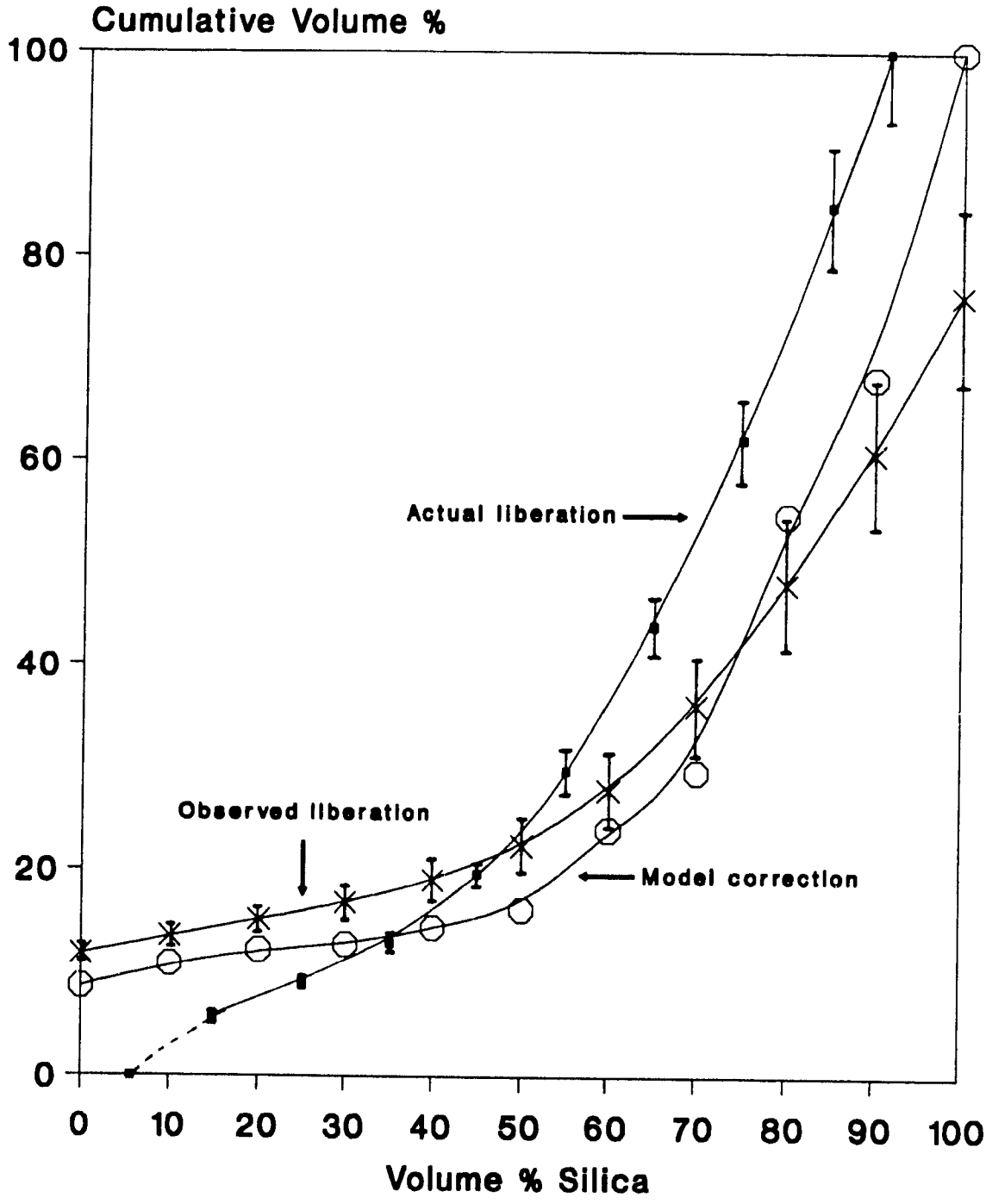

Figure 6.17 : Grade - recovery curves of actual liberation, observed liberation and model correction.

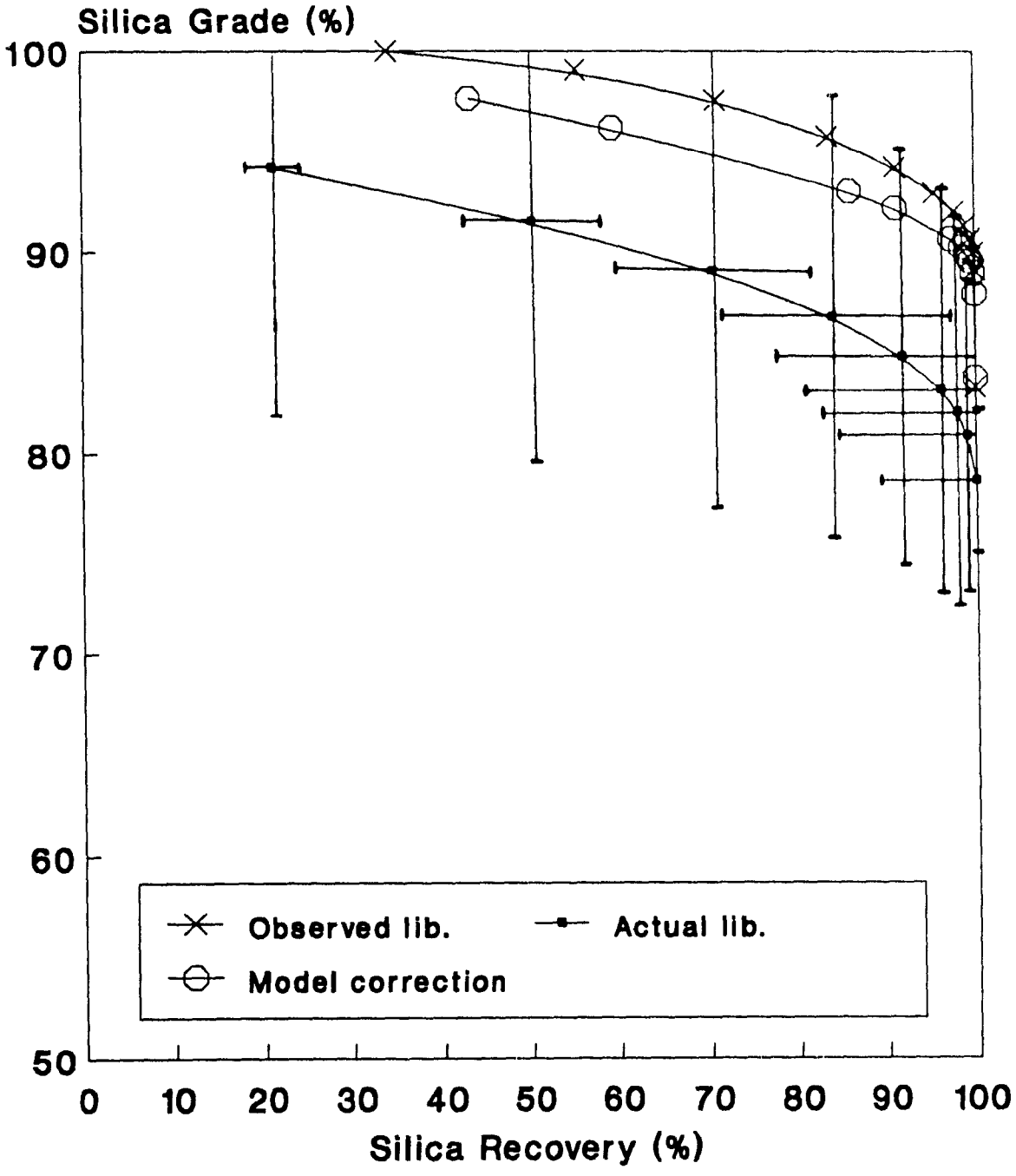

recovery curves. This figure is provided so that the information is summarized in a form familiar to mineral processing engineers [28]. The calculation of the grade and recovery have increased the size of the error bars [25](see Appendix A.6).

As mentioned earlier (Section 3.2.1), the actual liberation distribution was expected to lie between the observed liberation distribution (liberation overestimation) and the results of the sphere model correction (liberation underestimation). As Figures 6.16 and 6.17 indicate, the actual liberation does not fall between these two limits. The assay of this sample from heavy liquid separation was 62.9 volume % silica; the image analysis assay was 69.9 volume % silica. This discrepancy can be accounted for by the same reasons outlined for the previous two samples, but in this case, matrix resin may have been mistaken for the mounting medium resin resulting in a decrease in resin observations and in an increased silica assay. Any error in the observed results will, of course, create problems in the sphere model corrected results.

There is clearly some question here as to the accuracy of the results raised by the lack of equivalence between the measured and image analysis calculated assays. Poor contrast between the matrix resin and mounting medium is one possible cause. Hill [9, p.130], however, has challenged equivalence as a criterion of the accuracy of the liberation analysis. His reasoning is that with such extensive image processing designed to preserve textural integrity, the assay is sure to change. By how much is not known.

7. CONCLUSIONS AND FUTURE WORK

The conclusions drawn from this work are as follows :

1) Silica and ERL-4221 epoxy resin were found to be suitable material to form the two phases of the standard material.

2) A compromise between the production of locked material and the production of simple locked material has been found with regard to the ratio of particle size to grain size. The best results were obtained when the ratio was 1:1.

3) A material has been created which can be used to test the effectiveness of liberation analysis procedures including stereological correction methods.

4) In the liberation analysis in this work, the results of the standard material did not quite match the sphere sectioning results mostly, it is suspected, due to inadequate contrast between the matrix resin and the mounting medium.

Future work on the development of an artificial standard material would involve:

1) Using a different grain material. A material with better fracturing and polishing properties than silica could be found and tested. If the grain material and matrix material had similar fracturing properties, random breakage would be promoted, thus creating more locked particles. A grain material with a higher density than that of silica would provide for more accurate heavy liquid separations (i.e. increase the tolerance in incremental density fractionation work).

2) Using a different matrix material. Although the resin used in this work proved to be adequate, a resin with fracture properties similar to the grain material would produce more random breakage.

3) Testing a different grinding method. The shatterbox did not permit direct grinding in liquid nitrogen. The silica/resin blocks had to be submerged in a liquid nitrogen bath and then moved from the bath to the shatterbox. Grinding directly in liquid nitrogen would have made the resin more brittle and would have produced more random breakage.

4) Using a resin filler in the silica/resin blocks. The particles of the grain material can be physically separated from each other in the silica/resin blocks by mixing hardened particles of matrix resin in with the grain material. This filler will become part of the matrix resin when the liquid

matrix resin is added. This will reduce the incidence of complex locking since the grain material in the silica/resin blocks will not be touching. The breakage of these blocks will likely result in particles that contain only one silica nucleus and thus be simple locked.

5) Creating larger standard material particles. The size of the standard material particles can be increased to about 150-212 μm (-65 +100 mesh) while still maintaining an adequate number of particle sections per polished surface for a 32 mm mold. The advantages of this would be to make heavy liquid separations more accurate and to lessen the effect of halos and small surface defects on the polished surface.

6) Creating a stereological correction method using the standard material. The standard material could be sectioned to yield a sectioning matrix that can be used to transform uncorrected liberation data.

REFERENCES

1. Meloy, T.P. "Liberation Theory - Eight, Modern, Usable Theorems," Int. J. Min. Proc., Vol. 13, 1984, pp. 313-324.

2. Gaudin, A.M. Principles of Mineral Dressing, McGraw-Hill, 1939, pp. 70-91.

3. Wills, B.A. Mineral Processing Technology, 4th ed., Pergamon Press, Toronto, 1988, p. 23.

4. Kelly, E.G. and Spottiswood, D.J. Introduction to Mineral Processing, John Wiley and Sons, 1982, pp. 315-316.

5. Wiegel, R.L. and Li, K. "A Random Model for Mineral Liberation by Size Reduction", Trans. AIME, Vol. 238, 1967, pp. 45-56.

6. Meloy, T.P. and Gotoh, K. "Liberation in a Homogeneous Two-Phase Ore", Int. J. Min. Proc., Vol. 14(1), 1985, pp. 45-56.

7. Lynch, A.J. Mineral Crushing and Grinding Circuits, Elsevier, 1977, Chap. 9.

8. Gy, P.M. Sampling of Particulate Materials, Elsevier, 1982.

9. Hill, G.S. Applications of Two-Dimensional Image Analysis to Mineral Liberation Studies, McGill University doctorate thesis, April, 1990.

10. Gomez, C.O., Rowlands, N., Finch, J.A and Wilhelmy, J.-F. "A Specimen Preparation Procedure for Automated Image Analysis," Process Mineralogy VIII, eds. D. Carson and A. Vassiliou, TMS-AIME, 1988, pp. 359-367.

11. Walker, D.A. and LeCheminant, G.M. "An Integrated Image and X-Ray Analysis System : Description and Techniques in a Multiple Use Laboratory", Mineralogical Association of Canada Short Course on Image Analysis Applied to Mineral and Earth Sciences, Ottawa, May, 1989, pp. 43-55.

12. Goldstein, J.I. et al. Scanning Electron Microscopy and X-Ray Microanalysis, Plenum Press, 1981, p. 17.

13. Reid, A.F., Gottlieb, P., MacDonald, K.J. and Miller, P.R. "QEM*SEM Image Analysis of Ore Minerals: Volume Fraction, Liberation and Observational Variances," Applied Mineralogy, eds. W.C. Park, D.M Hausen and R.D. Hagni, 1984, pp.191-204.

14. Petruk, W. "Image Analysis of Minerals," Mineralogical Association of Canada Short Course on Image Analysis Applied to Mineral and Earth Sciences, Ottawa, May, 1989, pp. 6-18.

15. Petruk, W. "Techniques for Performing Image Analysis Routines," Mineralogical Association of Canada Short Course on Image Analysis Applied to Mineral and Earth Sciences, Ottawa, May, 1989, pp. 19-34.

16. Jones, M.P. and Horton, R. "Recent Developments in the Stereological Assessment of Composite (Middling) Particles by Linear Measurements," Proc. 11th Commonwealth Min. Metall. Congress, Hong Kong (ed. M.P. Jones), I.M.M. 1978, pp. 113-122.

17. Hill, G.S., Rowlands, N. and Finch, J. "Data Correction in Two-Dimensional Liberation Studies," Process Mineralogy VII, eds. A. Vassiliou, D. Hausen and D. Carbon, 1987, pp. 617-632.

18. Baba, K., Miller, J.D. and Herbst, J.A. "A General Transformation Function for the Prediction of Volumetric Abundance from Linear Grade Distributions," Annual AIME Meeting, New York, 1985.

19. Barbery, G. "Nouvelle Methode pour Caracteriser la Liberation Minerale par Analyses d'Images au Moyen de Mesures dans l'Espace a Une et Deux Dimensions. Theorie et Exemple d'Applications," XV Congres Int. de Mineralurgie, Cannes, 1985, Tome 1, pp. 20-30.

20. Miller, J.D. and Lin, C.L. "Treatment of Polished Section Data for Detailed Liberation Analysis," Int. J. Min. Proc., Vol. 22, 1988, pp. 41-58.

21. Barbery, G. "Latest Developments in the Interpretation of Section Measurements for Liberation," CSIRO and AMIRA workshop, Australia, March, 1989.

22. Bagga, P.S. Simulation of the Liberation Phenomena in Mineral Systems, Pennsylvania State University doctorate thesis, March, 1983.

23. Gabriel, B.L. S.E.M.: A User's Manual for Materials Science, American Society for Metals, Metals Park, Ohio, 1985, p. 149.

24. Petruk, W., CANMET, personal communication, 1991.

25. Adorjan, L.A. "Accumulation of Errors in Float and Sink Analysis," Proc. XVI International Mineral Processing Congress, Stockholm 1988, ed. P. Forssberg, Elsevier, 1988, pp. 1633-1644.

26. Schildknecht, C.E. and Skeist, I., ed. Polymerization Processes, John Wiley and Sons, Toronto, 1977, p. 598.

27. Jones, M.P. Applied Mineralogy : A Quantitative Approach, Graham and Trotman, Oxford, 1987, p. 73.

28. Finch J.A. and Gomez, C.O. "Separability Curves from Image Analysis Da' ," Minerals Engineering, Vol. 2, No. 4, 1989, pp. 565-568.

APPENDIX A

Grain Size : 600-850 µm Matrix Resin : Doped Epofix		
Particle Size Range (µm)	Mass (g)	Mass %
> 75	292.2	65.4
38 - 75	48.9	10.9
< 38	105.7	23.7
Total :	446.8	100.0

Appendix A.1 : Particle size distribution of 600-850 µm silica and doped Epofix crushed blocks.

Grain Size : 38-53 μm Matrix Resin : Epofix		
Particle Size Range (μm)	Mass (g)	Mass %
106 - 212	43.2	13.7
75 - 106	13.4	4.2
53 - 75	18.2	5.8
38 - 53	74.0	23.4
< 38	167.2	52.9
Total :	316.0	100.0

Appendix A.2 : Particle size distribution of 38-53 μm silica and Epofix crushed blocks.

Grain Size : 75-106 μm Matrix Resin : Doped Epofix		
Particle Size Range (μm)	Mass (g)	Mass %
106 - 212	36.0	9.1
75 - 106	95.8	24.3
53 - 75	70.2	17.8
38 - 53	46.6	11.8
< 38	145.2	36.9
Total :	393.8	100.0

Appendix A.3 : Particle size distribution of 75-106 μm silica and doped Epofix crushed blocks.

Grain Size : 38-53 µm Matrix Resin : ERL-4221		
Particle Size Range (µm)	Mass (g)	Mass %
106 - 212	38.1	18.5
75 - 106	11.9	5.8
53 - 75	15.3	7.4
38 - 53	42.9	20.8
< 38	97.9	47.5
Total :	206.1	100.0

Appendix A.4 : Particle size distribution of 38-53 µm silica and ERL-4221 crushed blocks.

Grain Size : 75-106 µm Matrix Resin : ERL-4221		
Particle Size Range (µm)	Mass (g)	Mass %
106 - 212	69.0	17.9
75 - 106	98.6	25.6
53 - 75	66.3	17.2
38 - 53	38.3	9.9
< 38	113.0	29.3
Total :	385.2	100.00

Appendix A.5 : Particle size distribution of 75-106 µm silica and ERL-4221 crushed blocks.

Appendix A.6

According to Adorjan, the errors associated with heavy liquid separations should be calculated thus :

Mass Percentage Error

An incremental heavy liquid analysis yields mass percentages $\Delta m_1, \Delta m_2, \ldots, \Delta m_i, \ldots \Delta m_n, \Delta m_{n+1}$ at densities $d_1, d_2, \ldots d_i, \ldots d_n$ (see figure below) with $a_1, a_2, \ldots a_i, \ldots a_n, a_{n+1}$ being the assay of each mass fraction. The reduced mass percent of the each fraction, i, is calculated thus :

$$\Delta M_i = abs\left[\frac{\Delta m_i}{(d_i - d_{i-1})}\right]$$

where d_0 = density of the lightest component of the feed

and d_{n+1} = density of the densest component of the feed.

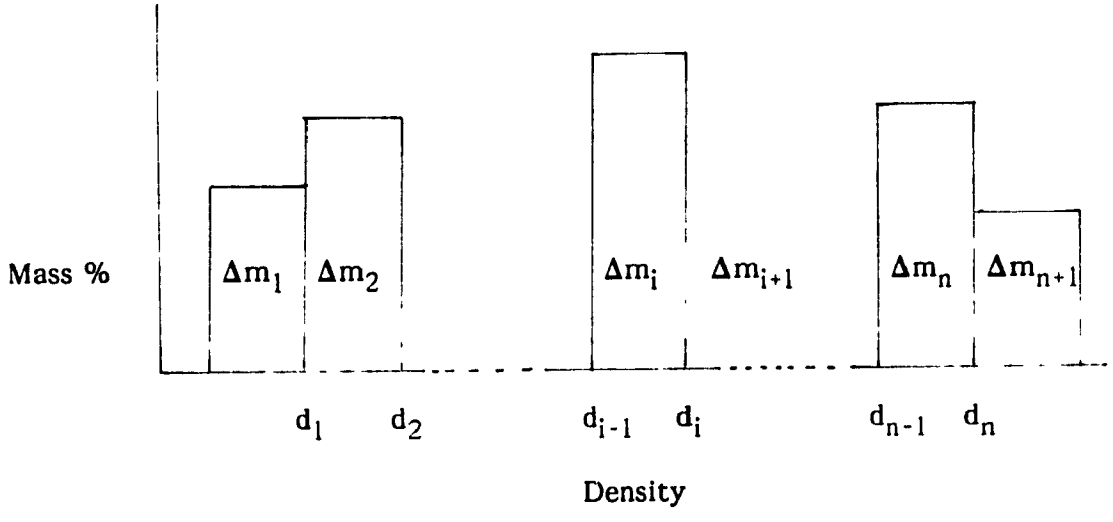

The absolute error of mass fraction i, due to a deviation in liquid density is:

$$e_{\Delta mdi} = abs\left[\delta d \frac{\Delta M_{i-1} + 2\Delta M_i + \Delta M_{i+1}}{2}\right]$$

with $\Delta M_0 = -\Delta M_1$ and $\Delta M_{n+2} = -\Delta M_{n+1}$ and where δd is the absolute error in liquid density.

Since the cumulative mass percent of the concentrate is :

$$m_j = \sum_{i=1}^{j} \Delta m_i$$

then the absolute error in the concentrate mass percent to fraction j is :

$$e_{mdj} = \sum_{i=1}^{j} e_{\Delta mdi}$$

Error in the Grade of the Density Fractions

The absolute error in the grade of a density fraction, e_{ai}, is the sum of three errors:

$$e_{ai} = \delta a_i + e_{api} + e_{adi}$$

where δa_i is the error in the assay of fraction i,

e_{api} is the error due to non-ideal separation,

e_{adi} is the error due to deviation in the density of the heavy liquid.

These three errors are as calculated below :

$$\delta a_i = \frac{\delta A}{a_i}$$

where δA is the relative error expressed as a percentage associated with the assay.

$$e_{api} = abs\left[\frac{0.742e_p^{\,2}}{\Delta m_i}\left((\Delta M_i+\Delta M_{i-1})\frac{a_i-a_{i-1}}{d_i-d_{i-2}} + (\Delta M_i+\Delta M_{i-1})\frac{a_{i+1}-a_i}{d_{i+1}-d_{i-1}}\right)\right]$$

with $\Delta M_0 = -\Delta M_1$ and $\Delta M_{n+2} = -\Delta M_{n+1}$ and where e_p is the probable error of float and sink analysis.

$$e_{adi} = abs\left[\delta d\,\frac{\Delta M_{i-1}+\Delta M_i}{2\Delta M_i}\left(\frac{a_i-a_{i-1}}{d_i-d_{i-2}}(d_{i-1}-d_{i-2}+\delta d)+a_{i-1}\right) + \delta d\,\frac{\Delta M_i+\Delta M_{i-1}}{2\Delta M_i}\left(\frac{a_{i+1}-a_i}{d_{i+1}-d_i}(d_i-d_{i-1}+\delta d)+a_i\right)\right]$$

Error in Concentrate Grade

The concentrate grade is :

$$c_j = \sum_{i=1}^{J} \Delta m_i a_i$$

The absolute error in the concentrate grade is calculated :

$$e_{cj} = c_j\left[\frac{\sum_{i=1}^{J}(e_{\Delta mdi}a_i+e_{ai}\Delta m_i)}{\sum_{i=1}^{J}\Delta m_i a_i} + \frac{e_{mdj}}{m_j}\right]$$

Error in Feed Grade

The feed grade is :

$$f = \frac{1}{100} \sum_{i=1}^{n} \Delta m_i a_i$$

The absolute error in the feed grade is calculated :

$$e_f = \frac{1}{100} \sum_{i=1}^{n} (e_{\Delta mdi} a_i + e_{ai} \Delta m_i)$$

Error in Recovery

The recovery is :

$$r_j = \frac{\sum_{i=1}^{j} \Delta m_i a_i}{f}$$

The absolute error in recovery is calculated :

$$e_{rj} = r_j \left[\frac{\sum_{i=1}^{j} (e_{\Delta mdi} a_i + e_{ai} \Delta m_i)}{\sum_{i=1}^{j} \Delta m_i a_i} + \frac{e_f}{f} \right]$$

Error Calculation Assumptions

The use of this error calculation technique required that some variables be assumed. The following assumptions were made : δd = 0.005 g/cm^3, δA = 0% (because no independent assay of the fractions was performed) and e_p = 0.005 g/cm^3. The calculation of the error of the grade of the density fractions, e_{ai}, was less than 1% for each fraction and thus was not indicated on the graphs.

APPENDIX B

Appendix B.1

The accuracy of the liberation analysis can be calculated by using the binomial distribution to estimate the relative error. If N particle sections are examined, let the probability of finding a section of a certian composition be p, while the probability of the failure to do so be q (i.e. q = 1 - p). The standard deviation, σ, on p for a binomial distribution is :

$$\sigma = \sqrt{\frac{pq}{N}} \qquad \text{B.1.1}$$

The acceptable error for quantitative results in most mineral processing applications is the 95% confidence interval which corresponds approximately to 2 standard deviations. The absolute error, e, is:

$$e = \pm 2\sqrt{\frac{pq}{N}} \qquad \text{B.1.2}$$

The relative error, E, is :

$$E = \frac{e}{p} \qquad \text{B.1.3}$$

Substituting equation B.1.2 into equation B.1.3, E (for a 95% confidence interval) is calculated thus :

$$E = \sqrt{\frac{4q}{pN}} \qquad \text{B.1.4}$$

N is known and p and q can be estimated from the data.

Since the liberation distribution was calculated in the image analysis, the error for each composition class varied according to the number of counts obtained from that class. Obviously, a high number of counts in a certain class would produce a result with a low error. The relative error for each composition class for each liberation distribution is calculated and tabulated with the image analysis data.

Appendix B.2 : Image Analysis of 45-55 vol.% Silica Standard Material

density of ERL-4221 resin = 1.21 g/cc
density of silica = 2.62 g/cc

Sample ST28A

Area of silica (microns^2) = 9020000
Area of resin (microns^2) = 10900000

Area percent silica = 45.3
Area percent resin = 54.7

Number of frames analyzed = 45
Number of particles analyzed = 5113

Volume % Silica Range	Volume % Silica of Total Sil.	Counts of Silica of Total Sil.	Area (um^2) Silica of Total Sil.	Volume % Particles	Area (um^2) Particles
0 - 10	0.31	207	27700	4.75	663000
10 - 20	1.07	143	97000	3.94	642000
20 - 30	2.82	194	254000	6.16	994000
30 - 40	6.01	252	542000	9.64	1538000
40 - 50	11.30	327	1020000	14.31	2270000
50 - 60	14.50	357	1310000	14.86	2390000
60 - 70	15.80	364	1430000	13.68	2204000
70 - 80	13.20	299	1200000	10.21	1589000
80 - 90	9.62	231	868000	6.60	1027000
90 -100	13.50	396	1210000	9.10	1263000
100	11.80	463	1060000	6.75	1065000
	99.93	3233	9018700	100.00	15645000

Volume % Resin Range	Volume % Resin of Total Res.	Counts of Resin of Total Res.	Area (um^2) Resin of Total Res.	Volume % Particles	Area (um^2) Particles
0 - 10	0.45	394	49300	7.41	1263000
10 - 20	1.46	230	159000	5.42	1025000
20 - 30	3.61	300	394000	8.35	1579000
30 - 40	7.11	363	774000	11.33	2202000
40 - 50	9.88	357	1080000	12.37	2380000
50 - 60	11.50	326	1250000	12.05	2270000
60 - 70	9.11	253	992000	8.07	1532000
70 - 80	6.74	191	735000	5.11	985000
80 - 90	4.66	135	507000	3.07	599000
90 -100	5.32	196	579000	3.50	604000
100	40.20	1880	4380000	23.34	4370000
	100.04	4625	10899300	100.00	18809000

For 45-55 vol.% sil. standard :

Volume % Silica Range	Silica Area (um^2)	Resin Area (um^2)	Total Area (um^2)	Area %	Cum. Area %	Freq.	Freq.%	Cum. Freq.%	Area % Relative Error (%)
0	0	4380000	4380000	21.99	21.99	1880	36.77	36.77	3.67
0 - 10	27700	579000	606700	3.05	25.04	207	4.05	40.82	13.62
10 - 20	97000	507000	604000	3.03	28.07	143	2.80	43.61	16.49
20 - 30	254000	735000	989000	4.97	33.03	194	3.79	47.41	14.08
30 - 40	542000	992000	1534000	7.70	40.74	252	4.93	52.34	12.28
40 - 50	1020000	1250000	2270000	11.40	52.13	327	6.40	58.73	10.70
50 - 60	1310000	1080000	2390000	12.00	64.13	357	6.98	65.71	10.21
60 - 70	1430000	774000	2204000	11.07	75.20	364	7.12	72.83	10.10
70 - 80	1200000	394000	1594000	8.00	83.20	299	5.85	78.68	11.22
80 - 90	868000	159000	1027000	5.16	88.36	231	4.52	83.20	12.86
90 -100	1210000	49300	1259300	6.32	94.68	396	7.74	90.94	9.65
100	1060000	0	1060000	5.32	100.00	463	9.06	100.00	8.86
	9018700	10899300	19918000	100.00		5113	100		

Appendix B.3 : Image Analysis of 75-85 vol.% Silica Standard Material

Sample ST27A

Area of silica (microns^2) = 15200000
Area of resin (microns^2) = 3850000

Area percent silica = 79.8
Area percent resin = 20.2

Number of frames analyzed = 49
Number of particles analyzed = 4749

Volume % Silica Range	Volume % Silica of Total Sil.	Counts of Silica of Total Sil.	Area (um^2) Silica of Total Sil.	Volume % Particles	Area (um^2) Particles
0 - 10	0.03	81	5030	0.79	140000
10 - 20	0.07	44	10900	0.42	75700
20 - 30	0.14	37	20600	0.46	82100
30 - 40	0.29	53	43900	0.70	125000
40 - 50	0.72	74	110000	1.37	244000
50 - 60	1.98	130	301000	3.01	537000
60 - 70	5.92	253	901000	7.68	1370000
70 - 80	13.40	450	2040000	15.10	2700000
80 - 90	22.00	609	3360000	22.10	3940000
90 -100	24.90	754	3790000	22.30	3970000
100	30.50	1340	4650000	26.10	4650000
	99.95	3825	15232430	100.03	17833800

Volume % Resin Range	Volume % Resin of Total Res.	Counts of Resin of Total Res.	Area (um^2) Resin of Total Res.	Volume % Particles	Area (um^2) Particles
0 - 10	4.68	752	180000	27.50	3970000
10 - 20	15.10	609	580000	27.20	3930000
20 - 30	17.20	453	663000	18.90	2720000
30 - 40	12.20	253	469000	9.48	1370000
40 - 50	6.00	127	231000	3.66	528000
50 - 60	3.59	77	138000	1.75	253000
60 - 70	2.10	53	80800	0.86	125000
70 - 80	1.58	36	60800	0.56	81200
80 - 90	1.66	43	64000	0.52	74900
90 -100	3.49	81	134000	0.97	140000
100	32.40	924	1250000	8.65	1250000
	100.00	3408	3850600	100.05	14442100

For 75-85 vol.% sil. standard :

Volume % Silica Range	Silica Area (um^2)	Resin Area (um^2)	Total Area (um^2)	Area %	Cum. Area %	Freq.	Freq.%	Cum. Freq.%	Area % Relative Error (%)
0	0	1250000	1250000	6.55	6.55	924	19.46	19.46	5.90
0 - 10	5030	134000	139030	0.73	7.28	81	1.71	21.16	22.03
10 - 20	10900	64000	74900	0.39	7.67	44	0.93	22.09	30.01
20 - 30	20600	60800	81400	0.43	8.10	37	0.78	22.87	32.75
30 - 40	43900	80800	124700	0.65	8.75	53	1.12	23.98	27.32
40 - 50	110000	138000	248000	1.30	10.05	74	1.56	25.54	23.07
50 - 60	301000	231000	532000	2.79	12.84	130	2.74	28.28	17.30
60 - 70	901000	469000	1370000	7.18	20.02	253	5.33	33.61	12.23
70 - 80	2040000	663000	2703000	14.16	34.18	450	9.48	43.08	8.97
80 - 90	3360000	580000	3940000	20.65	54.83	609	12.82	55.91	7.57
90 -100	3790000	180000	3970000	20.80	75.63	754	15.88	71.78	6.68
100	4650000	0	4650000	24.37	100.00	1340	28.22	100.00	4.63
	15232430	3850600	19083030	100.00		4749	100.00		

Appendix B.4 · Sectioning of 50 and 80 Vol.% Spheres

Volume % Silica Range	50 Vol.% A Spheres (Cum. Area%)	80 Vol.% A Spheres (Cum. Area%)
0	5.83	0.97
< 5	7.58	1.27
< 15	10.58	1.80
< 25	14.92	2.34
< 35	21.66	3.31
< 45	34.64	4.73
< 55	65.36	7.28
< 65	78.34	12.48
< 75	85.08	28.85
< 85	89.42	60.81
< 95	92.42	74.41
<100	94.17	81.11
100	100.00	100.00

Appendix B.5 : Sphere Sectioning Correction (Hill et al.)

If T = (nx1) matrix representing the true liberation distribution.
O = (nx1) matrix representing the observed liberation distribution (i.e. sectioning results).
S = (nxn) sectioning matrix This matrix represents the results of the sectioning of particles of known composition. The results of the random sectioning of two-phase spheres with planar interfaces and simple locking are shown below.

ACTUAL PARTICLE COMPOSITION

		Free A	0-10	10-20	20-30	30-40	40-50	50-60	60-70	70-80	80-90	90-100	Free B
	Free A	100.00	52.21	24.06	16.10	10.99	7.44	4.71	2.83	1.51	0.64	0.12	0.00
O P C	0-10	0.00	30.02	17.82	9.95	6.49	4.10	2.72	1.55	0.86	0.37	0.07	0.00
B A O	10-20	0.00	13.56	29.68	13.29	7.42	4.67	2.82	1.71	0.89	0.38	0.06	0.00
S R M	20-30	0.00	2.33	17.82	28.03	12.73	6.99	4.01	2.35	1.21	0.48	0.09	0.00
E T P	30-40	0.00	0.83	4.85	17.58	27.84	13.27	6.60	3.59	1.79	0.66	0.13	0.00
R I O	40-50	0.00	0.39	2.13	5.76	16.19	28.20	14.48	6.31	3.04	1.12	0.22	0.00
V C S	50-60	0.00	0.22	1.12	3.04	6.31	14.48	28.20	16.19	5.76	2.13	0.39	0.00
E L I	60-70	0.00	0.13	0.66	1.79	3.59	6.60	13.27	27.84	17.58	4.85	0.83	0.00
D E T	70-80	0.00	0.09	0.48	1.21	2.35	4.01	6.99	12.73	28.03	17.82	2.33	0.00
I	80-90	0.00	0.06	0.38	0.89	1.71	2.82	4.67	7.42	13.29	29.68	13.56	0.00
O	90-100	0.00	0.07	0.37	0.86	1.55	2.72	4.10	6.49	9.95	17.82	30.02	0.00
N	Free B	0.00	0.12	0.64	1.51	2.83	4.71	7.44	10.99	16.10	24.06	52.21	100.00

By definition :

$$O = S * T$$

Since O and S are known, T can be found thus :

$$T = \text{inverse } S * O$$

Appendix B.6 : Image Analysis of Standard Material Natural Distribution

Sample ST26A

Area of silica (microns^2) = 11300000
Area of resin (microns^2) = 4860000

Area percent silica = 69.9
Area percent resin = 30.1

Number of frames analyzed = 45
Number of particles analyzed = 4271

Volume % Silica Range	Volume % Silica of Total Sil.	Counts of Silica of Total Sil.	Area (um^2) Silica of Total Sil.	Volume % Particles	Area (um^2) Particles
0 - 10	0.12	113	13400	1.95	279000
10 - 20	0.39	77	44100	2.04	291000
20 - 30	0.55	70	61800	1.78	255000
30 - 40	1.13	88	128000	2.54	363000
40 - 50	2.15	104	244000	3.78	541000
50 - 60	4.36	163	493000	6.23	891000
60 - 70	7.72	221	874000	9.36	1340000
70 - 80	12.70	313	1430000	13.30	1910000
80 - 90	15.50	367	1760000	14.40	2060000
90 -100	21.30	535	2410000	17.60	2520000
100	34.10	1170	3850000	27.00	3850000
	100.02	3221	11308300	99.98	14300000

Volume % Resin Range	Volume % Resin of Total Res.	Counts of Resin of Total Res.	Area (um^2) Resin of Total Res.	Volume % Particles	Area (um^2) Particles
0 - 10	2.18	535	106000	20.30	2500000
10 - 20	6.30	367	306000	16.80	2050000
20 - 30	9.75	315	474000	15.50	1910000
30 - 40	9.61	221	467000	10.90	1340000
40 - 50	8.08	160	393000	7.14	879000
50 - 60	6.20	107	301000	4.45	548000
60 - 70	4.70	87	229000	2.87	353000
70 - 80	4.19	70	204000	2.19	269000
80 - 90	4.45	72	216000	2.07	255000
90 -100	5.52	114	269000	2.29	282000
100	39.00	1050	1900000	15.40	1900000
	99.98	3098	4865000	99.91	12286000

Observed natural liberation distribution :

Volume % Silica Range	Silica Area (um^2)	Resin Area (um^2)	Total Area (um^2)	Area %	Cum. Area %	Freq.	Freq.%	Cum. Freq %	Area % Relative Error (%)
0	0	1900000	1900000	11.75	11.75	1050	24.58	24.58	5.36
0 - 10	13400	269000	282400	1.75	13.49	113	2.65	27.23	18.56
10 - 20	44100	216000	260100	1.61	15.10	77	1.80	29.03	22.59
20 - 30	61800	204000	265800	1.64	16.75	70	1.64	30.67	23.71
30 - 40	128000	229000	357000	2.21	18.95	88	2.06	32.73	21.10
40 - 50	244000	301000	545000	3.37	22.32	104	2.44	35.17	19.37
50 - 60	493000	393000	886000	5.48	27.80	163	3.82	38.98	15.36
60 - 70	874000	467000	1341000	8.29	36.09	221	5.17	44.16	13.10
70 - 80	1430000	474000	1904000	11.77	47.86	313	7.33	51.49	10.88
80 - 90	1760000	306000	2066000	12.77	60.64	367	8.59	60.08	9.98
90 -100	2410000	106000	2516000	15.56	76.20	535	12.53	72.61	8.09
100	3850000	0	3850000	23.80	100.00	1170	27.39	100.00	4.98
	11308300	4865000	16173300	100.00		4271	100.00		

Volume % Silica Range	Volume Silica Recovery (%)	Cum. Vol. Sil. Recovery (%)	Grade Silica
0	0.00	100.00	83.28
0 - 10	0.13	100.00	89.05
10 - 20	0.35	99.87	89.92
20 - 30	0.59	99.53	90.63
30 - 40	1.11	98.94	91.26
40 - 50	2.18	97.83	91.99
50 - 60	4.32	95.66	92.92
60 - 70	7.73	91.33	94.17
70 - 80	12.67	83.60	95.72
80 - 90	15.58	70.93	97.55
90 -100	21.20	55.36	99.08
100	34.15	34.15	100.00
	100.00		

Actual Natural Distribution :

62.9 vol.% sil and 37.1 vol.% res.

Volume % Silica Range	Vol. %	Cum. Vol. %	Volume Silica Recovery (%)	Cum. Vol. Sil. Recovery (%)	Grade Silica
0	0.00	0.00	0.00	100.00	78.66
0 -5.6	0.00	0.00	0.00	100.00	78.66
5.6 - 15	5.63	5.63	0.92	100.00	78.66
15 - 25	3.41	9.05	1.08	99.08	80.88
25 - 35	3.79	12.83	1.80	97.99	82.06
35 - 45	6.76	19.60	4.30	96.19	83.16
45 - 55	10.06	29.66	7.99	91.90	84.78
55 - 65	14.15	43.81	13.48	83.91	86.75
65 - 75	18.21	62.02	20.23	70.43	89.05
75 - 85	22.86	84.88	29.03	50.20	91.51
85 -91.	15.12	100.00	21.17	21.17	94.19
91. -100	0.00	100.00	0.00	0.00	
100	0.00	100.00	0.00	0.00	
	100.00		100.00		

Sphere Corrected Natural Distribution

Volume % Silica Range	Vol. %	Cum. Vol. %	Volume Silica Recovery (%)	Cum. Vol. Sil. Recovery (%)	Grade Silica
0	8.63	8.63	0.00	100.00	83.71
0 - 10	2.18	10.81	0.16	100.00	87.88
10 - 20	1.34	12.15	0.28	99.84	88.93
20 - 30	0.53	12.67	0.19	99.56	89.49
30 - 40	1.64	14.31	0.81	99.37	89.68
40 - 50	1.78	16.09	1.14	98.56	90.18
50 - 60	7.81	23.90	6.11	97.42	90.61
60 - 70	5.69	29.59	5.26	91.32	92.15
70 - 80	24.99	54.58	26.64	86.06	93.00
80 - 90	13.46	68.04	16.26	59.41	96.16
90 -100	31.96	100.00	43.16	43.16	97.63
100	0.00	100.00	0.00	0.00	
	100.00		100.00		